AD-A126 380 ULTRASONIC NON-DESTRUCTIVE TESTING OF COMPOSITE MATERIALS(U) CORNELL UNIV ITHACA NY DEPT OF THEORETICAL AND APPLIED MECHANICS W SACHSE ET AL. 08 FEB 83 1/1

UNCLASSIFIED AFOSR-TR-83-0150 F49620-78-C-0100 F/G 14/2 NL

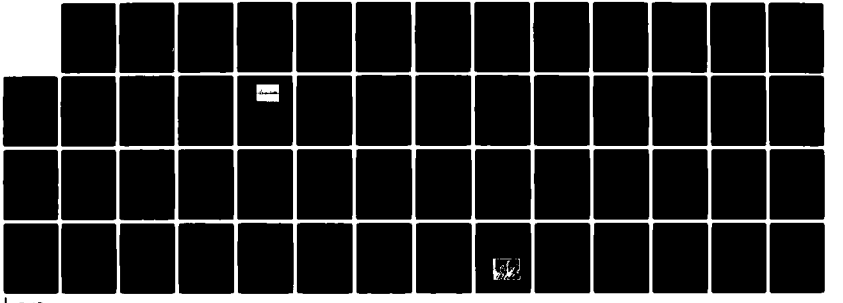

END
DATE FILMED
4 83
DTIC

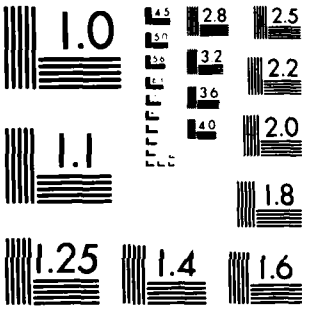

(13)

ULTRASONIC NON-DESTRUCTIVE TESTING OF COMPOSITE MATERIALS

Final Report to the

Air Force Office of Scientific Research

by

Wolfgang Sachse and Yih-Hsing Pao

Department of Theoretical and Applied Mechanics

Cornell University, Ithaca, New York - 14853

CONTRACT NO. F49620 - 78 - C - 0100

February 8, 1983

UNCLASSIFIED

SECURITY CLASSIFICATION OF THIS PAGE (When Data Entered)

REPORT DOCUMENTATION PAGE		READ INSTRUCTIONS BEFORE COMPLETING FORM
1. REPORT NUMBER **AFOSR-TR- 83-0150**	2. GOVT ACCESSION NO. AD-A126380	3. RECIPIENT'S CATALOG NUMBER
4. TITLE (and Subtitle) ULTRASONIC NON-DESTRUCTIVE TESTING OF COMPOSITE MATERIALS		5. TYPE OF REPORT & PERIOD COVERED FINAL 1 Aug 78 - 28 Feb 82
		6. PERFORMING ORG. REPORT NUMBER
7. AUTHOR(s) WOLFGANG SACHSE YIH-HSING PAO		8. CONTRACT OR GRANT NUMBER(s) F49620-78-C-0100
9. PERFORMING ORGANIZATION NAME AND ADDRESS CORNELL UNIVERSITY DEPT OF THEORETICAL & APPLIED MECHANICS ITHACA, NY 14853		10. PROGRAM ELEMENT, PROJECT, TASK AREA & WORK UNIT NUMBERS 61102F 2307/B2
11. CONTROLLING OFFICE NAME AND ADDRESS AIR FORCE OFFICE OF SCIENTIFIC RESEARCH/NA BOLLING AFB, DC 20332		12. REPORT DATE February 1983
		13. NUMBER OF PAGES 51
14. MONITORING AGENCY NAME & ADDRESS(if different from Controlling Office)		15. SECURITY CLASS. (of this report) Unclassified
		15a. DECLASSIFICATION DOWNGRADING SCHEDULE

16. DISTRIBUTION STATEMENT (of this Report)

Approved for Public Release; Distribution Unlimited.

17. DISTRIBUTION STATEMENT (of the abstract entered in Block 20, if different from Report)

18. SUPPLEMENTARY NOTES

19. KEY WORDS (Continue on reverse side if necessary and identify by block number)

NON-DESTRUCTIVE TESTING
COMPOSITE MATERIALS
ULTRASONICS
DISPERSION
ATTENUATION

20. ABSTRACT (Continue on reverse side if necessary and identify by block number)

This final technical report summarizes the work completed on a project utilizing ultrasonic wave dispersion, frequency-dependent velocities and attenuation measurements in a variety of composite materials. The report summarizes various measurement techniques and makes a critical comparison between the results obtained using each of the techniques on various composite specimens and pure epoxy matrix only. The use of such measurements as a technique for monitoring the microstructural changes

DD FORM 1 JAN 73 1473 EDITION OF 1 NOV 65 IS OBSOLETE

UNCLASSIFIED

SECURITY CLASSIFICATION OF THIS PAGE (When Data Entered)

accompanying the mechanical deformations and thermal cyclings of a composite specimen is investigated. The measurements from 1 to 10 MHz clearly show an increase in attenuation, however, the variation from specimen to specimen and between the values obtained with the various techniques is greater than the microstructurally induced attenuation changes. The effects on the dispersion curve and the frequency-dependent velocity data is less than the variation measured from specimen to specimen.

1.0 INTRODUCTION

This final scientific report gives an overview of the work completed under AFOSR Contract #F49620-78-C-100 dealing with the ultrasonic non-destructive testing of composite materials. Briefly summarized are the results obtained in the first two years of this project while the work completed in the third and final year of the contract is described in more detail. The project was originally scheduled as a two-year program from August 1, 1978 through July 31, 1980 . However, the original contract was amended to continue funding for one more year through July 31, 1981. Later, a no-cost extension to February 28, 1982 was granted.

The overall objective of this program has been to investigate experimentally and theoretically the dispersion and attenuation of ultrasonic waves in various composite materials. The research program was designed to explore the influence of microstructural and material property effects on the propagation of elastic waves through a composite material. Various experimental techniques were also to be evaluated by which ultrasonic wave dispersion effects could be measured to determine whether such measurements could be utilized as a new ultrasonic NDT tool for the inspection of structures fabricated from composite materials. Answers to these questions were to be obtained by carrying out the following six tasks:

1. Ultrasonic wave dispersion measurements were to be conducted in several uni-directional and cross-plied laminates of graphite-epoxy specimens.

2. Continuous and pulsed ultrasonic wave measurements were to be carried out on graphite-epoxy laminates. Investigation was to be made to obtain a quantitative characterization of the dissipative behavior and the separation of the attenuation of ultrasonic waves due to dispersion and dissipation.

3. The quantitative damping behavior of several laminates was to be measured by phase spectra techniques.

4. Models were to be developed to make predictions of the dispersion and dissipation behavior of laminates which were used in the experiments. Comparison was to be made between the calculations and the experimental results.

5. The use of multiple scattering analyses was to be investigated to determine the damping resulting from the presence of microstructural features in laminates.

6. Measurements of the dispersive and dissipative properties were to be made on composite specimens to determine the effects of mechanical loading and/or environmental exposure conditions.

2.0 PROJECT OVERVIEW

2.1 Work Summary

In work completed under a previous AFOSR contract, it was shown that the dispersion relation, $k(f)$, and the frequency-dependent phase and group velocities of ultrasonic waves can be determined with the method of ultrasonic phase spectroscopy. Details of the technique have been published [1,2], so it suffices to repeat here only the essentials of the technique. In the technique, the frequency-dependent wavenumber, $k(f)$, (or a material's dispersion relation) is found directly from determination of the Fourier phase spectrum, $\phi(f)$, of a broadband ultrasonic pulse which has propagated through a specimen of thickness, L. The dispersion relation is

$$k(f) = [\phi_o - \phi(f)]/L + 2\pi f\tau_s/L \qquad (1)$$

In this equation, $\phi(f)$, is the initial phase constant and τ_s is a time-delay constant, both constants are determined in a particular testing

configuration. From the dispersion relation follow the phase velocity, c(f), and the group velocity, v(f)

$$c(f) = 2\pi f/k(f) \tag{2}$$

$$v(f) = 2\pi(\partial f/\partial k) \tag{3}$$

The experimental work completed in the first two years has utilized this method to make measurements on various composite material specimens. The work completed in the first two years has been described in detail in two Interim Reports, dated October 1979 and December 1980, respectively. It is only briefly summarized here.

The research conducted in the first year included:

1. Ultrasonic dispersion measurements in uni-directional and cross-plied laminates of graphite/epoxy and boron/epoxy specimens were made.
2. The attenuation and dissipation of ultrasonic waves was measured in composite materials.
3. An integral relation between the attenuation coefficient and the dispersion relation (frequency-dependent phase velocity) was developed for viscoelastic waves using the Kramers-Kronig relation.
4. The scattering of elastic and viscoelastic waves in a laminated composite specimen was analyzed.

The results obtained in the first year showed that ultrasonic dispersion measurements could be made in uni-directional as well as cross-plied laminate specimens of graphite/epoxy. The wave propagation in the frequency range from 1 to 20 MHz was found to be essentially non-dispersive. In a composite specimen which exhibits dispersion (such as specific directions in specimens of boron/epoxy), very slight changes in the dispersion became apparent with

thermal treatments of the specimen, but the connection between the ultrasonic measurements and specific microstructural changes was not clear.

Various techniques for measuring the frequency dependence of ultrasonic attenuation of ultrasonic longitudinal and shear wave modes were implemented. Attenuation measurements were completed in various specimens of graphite/epoxy and boron/epoxy.

The theory of ultrasonic phase spectroscopy was extended with Hilbert transforms to permit the determination of the dispersion-related attenuation of ultrasonic waves in composite materials. A computer algorithm for performing such determinations was developed and it was tested with theoretical waveforms expected for a model viscoelastic material (Voigt solid).

A statistical multiple scattering theory was developed to analyze the propagation of waves normal to a layered structure consisting of elastic and viscoelastic materials which modelled a laminated composite material. The results showed that "stop bands" existed and that it was possible, in principle, to delineate between the scattering losses and the viscoelastic losses in such a material by noting the behavior of the frequency-dependence of the attenuation outside of the stop band.

In the second year the additional research was conducted on the following topics:

1. Ultrasonic dispersion and attenuation measurements were completed on specimens of unreinforced epoxy resin and cross-plied graphite/epoxy.

2. Two new ultrasonic techniques were developed and implemented for making ultrasonic attenuation measurements in composite specimens.

3. A critical comparison was begun of the various techniques for measuring the frequency-dependent attenuation in composite material specimens.

4. Experiments to determine the detectability of deformation-induced microstructural changes in cross-plied graphite/epoxy specimens with ultrasonic dispersion and attenution measurements were started.

5. The mathematical foundation of the Kramers-Kronig relation and its use for processing ultrasonic dispersion data was investigated.

Thus, in the second year of this project additional wave dispersion and frequency-dependent ultrasonic attenuation measurements were completed in specimens of graphite/epoxy. There was general agreement between these new measurements and those made previously. For quantitative comparisons between the measurements, least-square-fit algorithms were implemented into the ultrasonic signal processing system which permitted fitting polynomial phase velocity and attenuation functions to the measured data points. Reproducible measurements in graphite/epoxy specimens were obtained with one technique.

In addition, two new frequency-dependent attenuation measurement techniques were implemented for measurements with composite material specimens. One is a modified, swept-frequency, continuous-wave technique in which the resonance peaks of a specimen are analyzed at various amplitude levels. The other technique utilizes the Kramers-Kronig relation to find the material attenuation from measurements of the wave dispersion, or vice versa with only a single echo requirement. A firm basis for the technique was developed and measurements with graphite/epoxy specimens were undertaken. The agreement between the various techniques was investigated. It was found that the attenuation determined via the Hilbert-transform technique differs

significantly from that determined by all the other techniques.

In the third year, additional ultrasonic wave dispersion and attenuation measurements were completed. Specifically, the folowing work was completed:

1. Ultrasonic measurements of several multi-layer laminates which were fabricated of elastic, viscoelastic or elastic layers in various configurations were completed.
2. Additional ultrasonic measurements were completed in 32-ply specimens of 0/90° cross-plied laminated graphite/epoxy (AS3501-5) which were subjected to mechanical loadings or repeated thermal treatments.

2.2 Participating Personnel

The research personnel who were supported during the first two years have been listed in the two earlier Interim Reports. During the last eighteen months of this contract, the following research personnel were supported:

1. Principal Investigator: W. Sachse (1 month)
2. Co-Principal Investigator: Y.H. Pao (1.5 months)

and the following research associates and assistants:

Post-doctoral associates -

3. R. Weaver (5 months)
4. F. Santosa (6 months)

Graduate student assistants--

5. P. Chen (7.5 months)
6. D. Koshoni (2.5 months)
7. P. Hsieh (2.5 months)
8. K. Ko (2 months)
9. T. Wu (5 months)

In addition, a temporary part-time research aide and a work-study student assissted in this research.

3.0 SUMMARY OF IMPLEMENTED EXPERIMENTAL TECHNIQUES

As proposed in the original proposal and as described in the two interim reports ot this project, various ultrasonic techniques were applied to measure the frequency-dependent ultrasonic attenuation in various composite specimens. The techniques which were used included:

1. Continuous-wave, swept-frequency technique
2. Radio-frequency (r.f.) burst technique
3. Broadband pulse analysis technique
4. Retlection coefficient method
5. Hilbert-transform technique

The first four of the aforementioned techniques are conventional ultrasonic techniques which have been used in various forms by other investigators. In the course of this work, the continuous-wave, swept-frequency technique (#1 above) was modified to enable it to be used to make measurements in highly absorbent and thick specimens, or in cases in which the specimen resonance peaks cannot be clearly resolved. As mentioned in Section 2, the Hilbert-transform technique (#5 above) was also developed and implemented in the course of the work carried out under this project. Since reference to the above techniques will be made later, each of them is briefly summarized here.

(1) Continuous-wave Resonance Technique - In this technique, continuous harmonic waves which are slowly varying in frequency, are launched into a specimen, with the transmitted signals detected with either the same or another transducer attached to the specimen. The resonance frequencies of the specimen are recorded and the damping determined from the half-power points on the resonance peak. As indicated in Section 2, in the second year of this contract, an important modification was developed which permitted the measurements to be made on resonance peaks on which the half-power points are not clearly identifiable. In this modification, a formula was derived which utilizes the resonance peak width measured at any power level to determine the damping characteristics of the specimen.

(2) R.F. Burst Method - In this technique, radio-frequency bursts of various center frequencies are transmitted through a specimen. Measurement of the logarithmic decay of at least two echoes, $V_1(t)$ and $V_2(t)$, gives the ultrasonic attenuation of the material at the center frequency, f_o, of the r.f. measurement burst, that is

$$\alpha(f_o) = 20/L \log \frac{V_1(t)}{V_2(t)} \qquad (4)$$

(3) Broadband Pulse-Echo Method - This method is a variation of the above, with broadband pulses, being used to make the measurements. Any two broadband echoes, $V_1(t)$ and $V_2(t)$, are Fourier-transformed into the frequency domain giving $\bar{V}_1(f)$ and $\bar{V}_2(f)$ from which the attenuation can be determined as a function of frequency according to

$$\alpha(f) = 20/L \log \frac{\bar{V}_1(f)}{\bar{V}_2(f)} \qquad (5)$$

(4) Reflection Coefficient Method - In this technique, a broadband pulse is reflected from an interface between a non-dispersive buffer rod and a composite material specimen. From analysis of specific echoes, the frequency-dependent interface reflection coefficient and attenuation coefficient is found for the specimen. Unfortunately, this technique appears to be very sensitive to the nature of the buffer-specimen interface.

(5) Hilbert-transform Technique - The Kramers-Kronig relations state that for electromagnetic waves propagating through a dielectric, the attenuation coefficient is related to the phase velocity of the wave by an integral involving the latter over all frequencies, and vice versa, thus corresponding to the Hilbert transform relationship between phase velocity and attenuation. Under this contract, a similar relation was developed for ultrasonic waves propagating through a viscoelastic or a composite material. The processing of only one echo yields the attenuation in this approach.

4.0 SUMMARY OF WORK COMPLETED IN THE LAST YEAR

In the last year of this contract, a critical comparison between the results obtained using various dispersion and attenuation measurement techniques was completed. As in our earlier work, oure epoxy specimens as well as graphite/epoxy specimens were measured. All measurements were repeated several times to clearly establish the variation between the measurements made on one specimen at either one location or at several locations in one specimen and the results obtained between the various measurement techniques.

In the following, the mean of the measured phase velocity or attenuation is plotted together with either the standard deviation curves or the diffraction-corrected curve in the frequency range from 0 to 10 MHz. For the velocity measurements, it was found that the coefficients of variation, σ_c , vary by no more than one percent, and for attenuation measurements, the coefficients of variation, σ_a , are within five percent. This indicates the reproducibility with which each set of measurements can be made. In the following, the results of measurements conducted on pure epoxy specimens, glass-laminated specimens, and 32-ply graphite/epoxy specimens will be described in detail.

4.1 Pure Epoxy Specimens

The results of ultrasonic measurements made on specimens of pure epoxy whose thickness was 0.5 cm to determine their frequency-dependent phase velocity and attenuation is described in this section.

(a) Phase velocity - An example of an input signal and the signal transmitted through the specimen are shown in Figures 1(a) and (b) respectively. The dispersion and phase velocity curves obtained via Eqs. 1 and 2 are shown in Figures 1(c) and (d), respectively. The measured phase velocity is generally higher than it should be at lower frequencies because of wave diffraction effects. Therefore, these were removed using the diffraction correction data of Benson, *et al* [3].

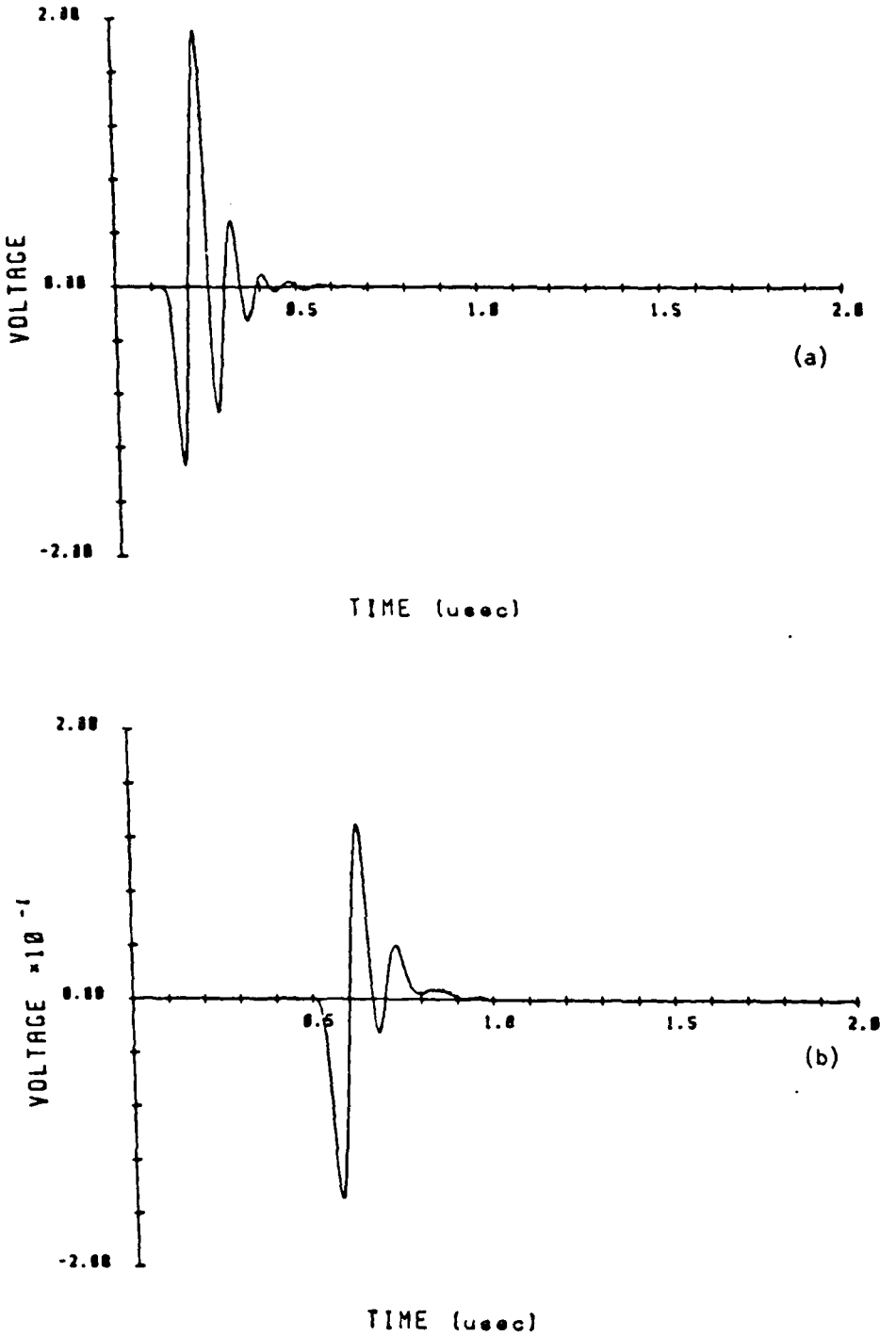

Figure 1. Signals of pure epoxy specimen for phase velocity measurements: (a) excitation signal, (b) delayed signal through the specimen (delayed time τ_s = 1.4 μsec)

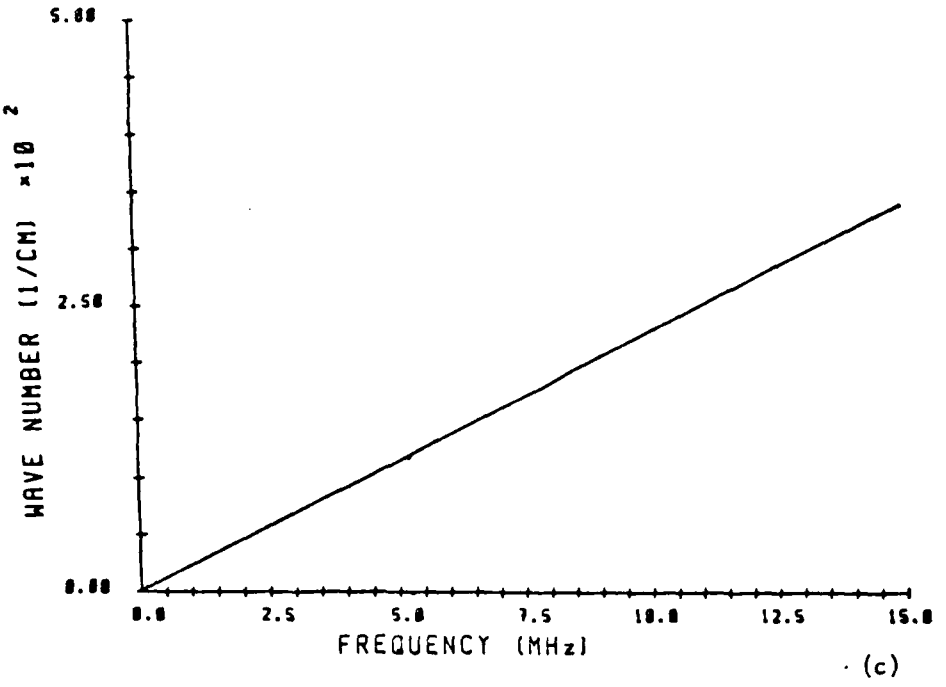

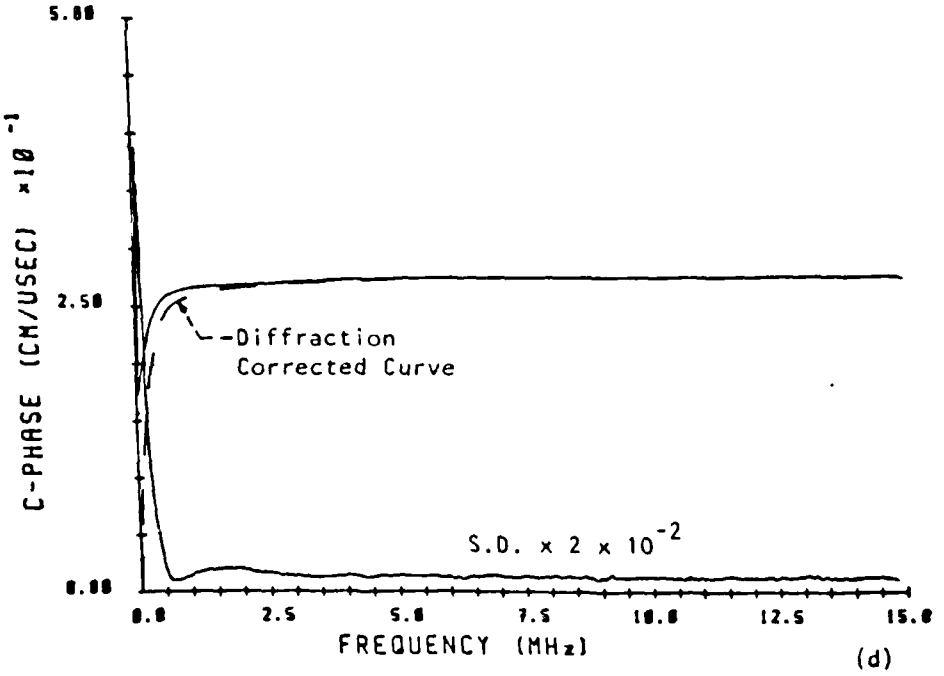

Figure 1. (c) dispersion relation, and (d) phase velocity and its standard deviation.

The dotted line in the phase velocity figure is the diffraction-corrected phase velocity. The standard deviation of phase velocity relative to the mean of each measuring set is shown in Figure 1(d). The phase velocity shows little dispersion for pure epoxy specimens in the frequency range from 0 to 10 MHz.

(b) Attenuation - A picture of narrow-band r.f. burst echoes propagating in a pure epoxy specimens is shown in Figure 2. The attenuation derived from these signals via Eq. 5 is also shown in Figure 2. In the figure, the solid line is the least-square fitted parabolic curve while the dashed line is the diffraction-corrected curve. The effect of the diffraction is to give a higher apparent attenuation.

The echoes obtained in a one-transducer, pulse/echo test with a half-inch diameter broadband transducer and the Fourier amplitude spectra are shown in Figures 3(a)-(c). The attenuation curve with its standard deviation curves are shown in Figure 3(d). The diffraction-corrected curve is shown in Figure 3(e). The results obtained in a pitch-catch or through-transmission measurement with quarter-inch diameter transducers are shown in Figure 4(a). Also shown in Figures 4 (a)-(c) are the respective Fourier amplitude spectra. The attenuation curve and its standard deviation curves are shown in Figure 4(d). Figure 4(e) shows the attenuation curve and the diffraction-corrected curve.

Application of the buffer rod method (using a 1/4 inch (0.635 cm) diameter transducer) yields the echos denoted as A, B, and C, and their Fourier amplitude spectra as shown in Figures 5(a)-(d). The reflection

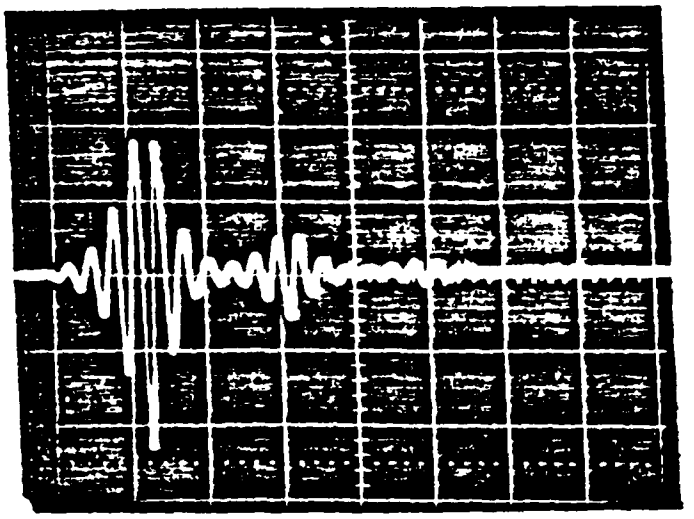

Figure 2. The r.f. burst signals with center frequency at 2.5 MHz.

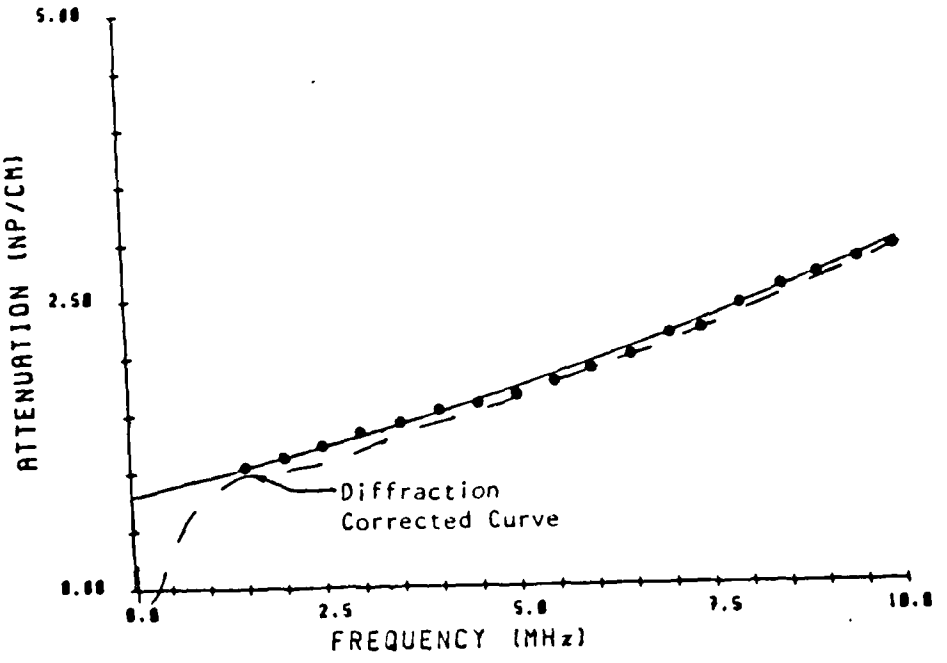

Figure 2 . The r.f. burst attenuation of pure epoxy specimen.

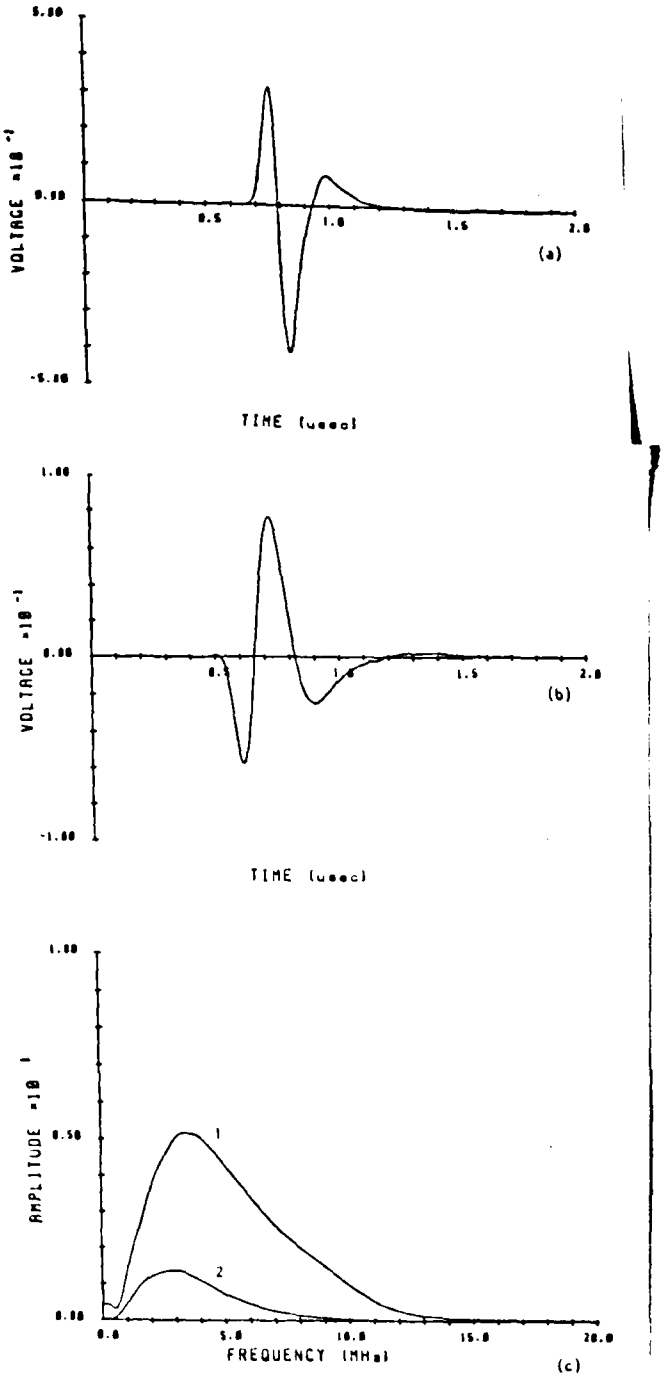

Figure 3. 1-transducer (1/2 inch diameter) signals of pure epoxy specimen for attenuation measurement: (a) echo 1. (b) echo 2, (c) Fourier amplitude spectra of echo 1 and 2.

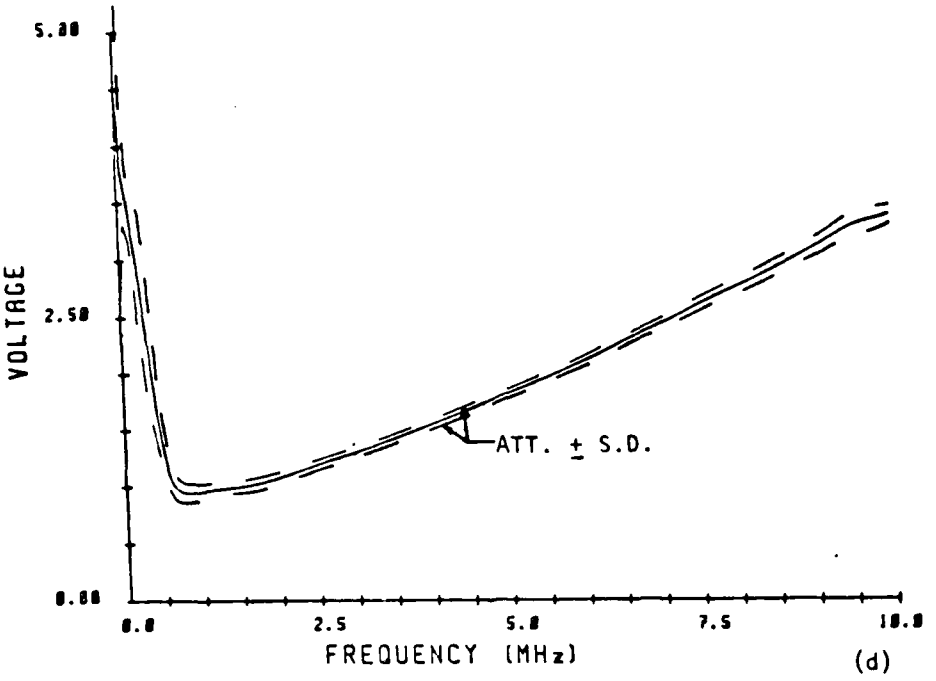

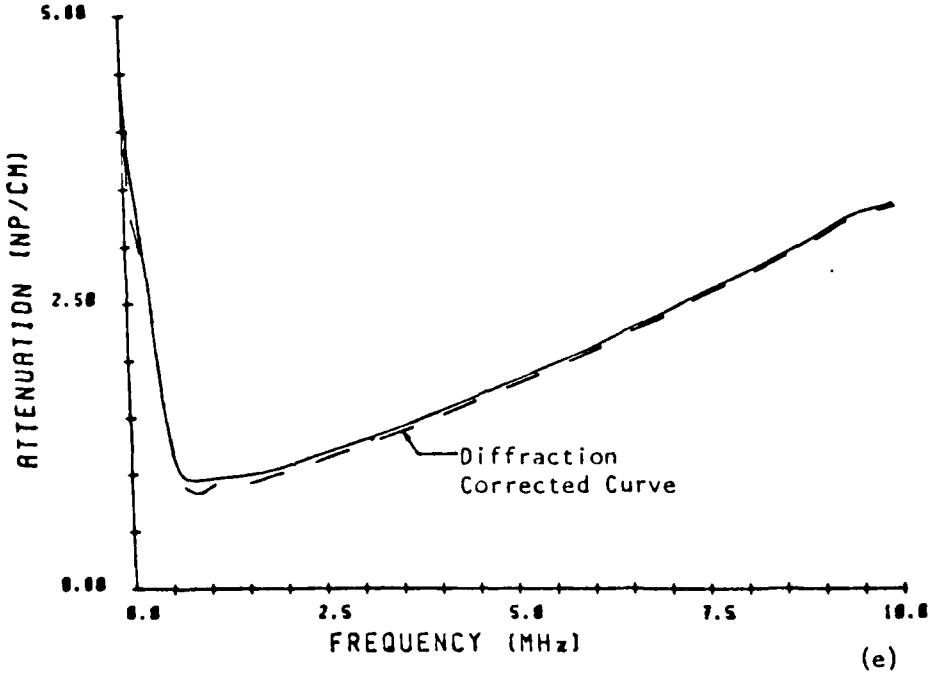

Figure 3. (d) attenuation and att. ± S.D., (e) attenuation and its diffraction corrected curve.

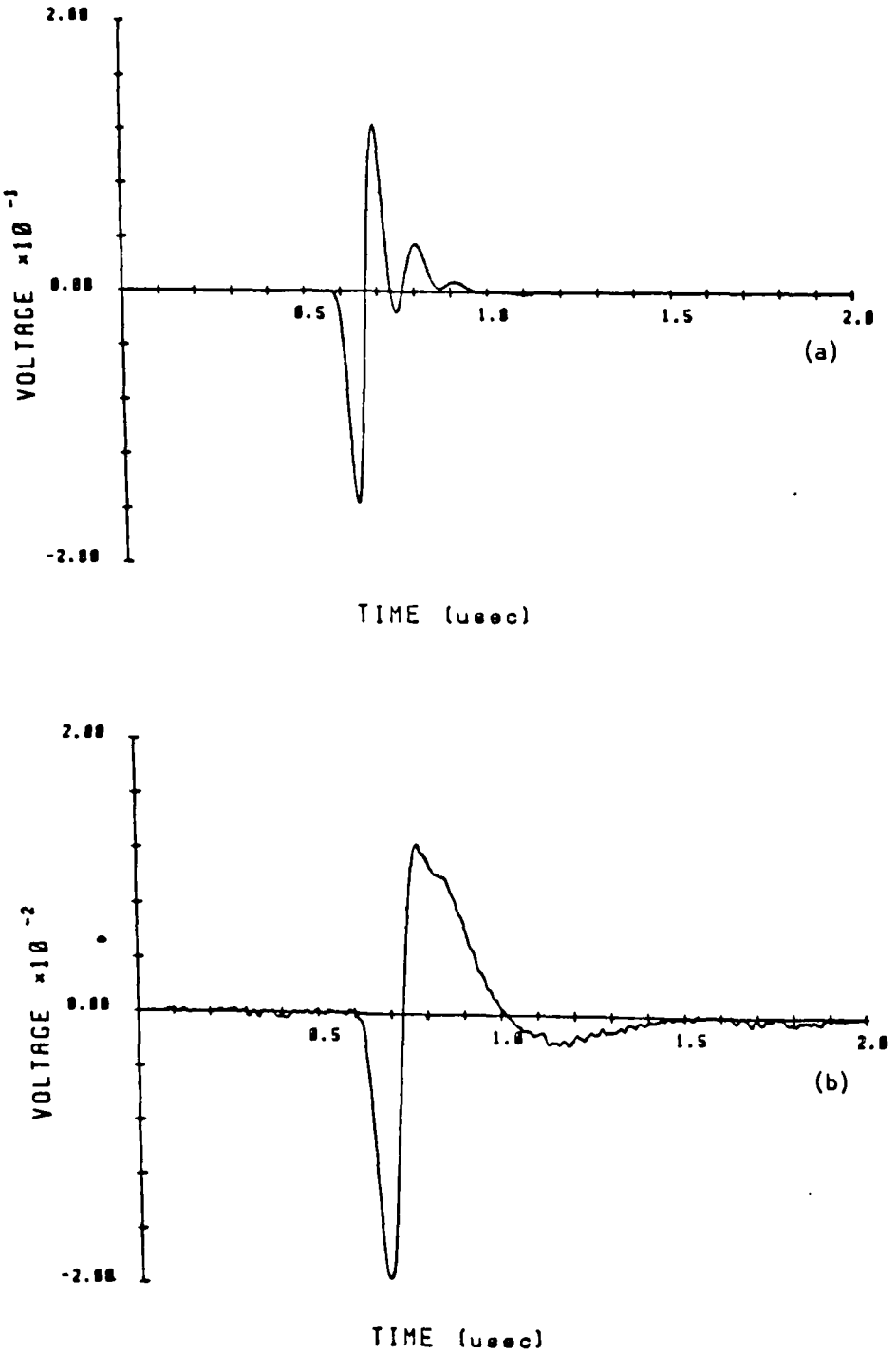

Figure 4. Through transmission signals of pure epoxy specimen for attenuation measurement: (a) echo 1, (b) echo 2.

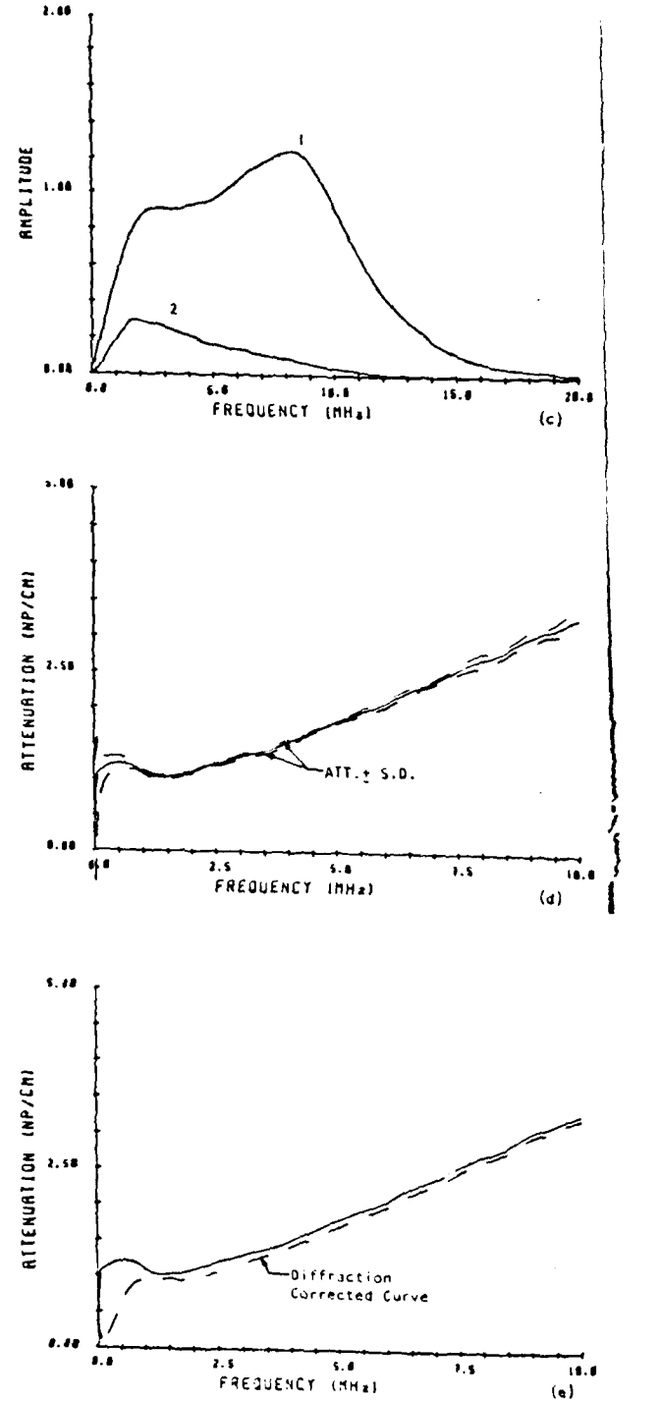

Figure 4. (c) Fourier amplitude spectra of echos 1 and 2,
(d) attenuation and att. ± S.D..
(e) attenuation and its diffraction corrected curve.

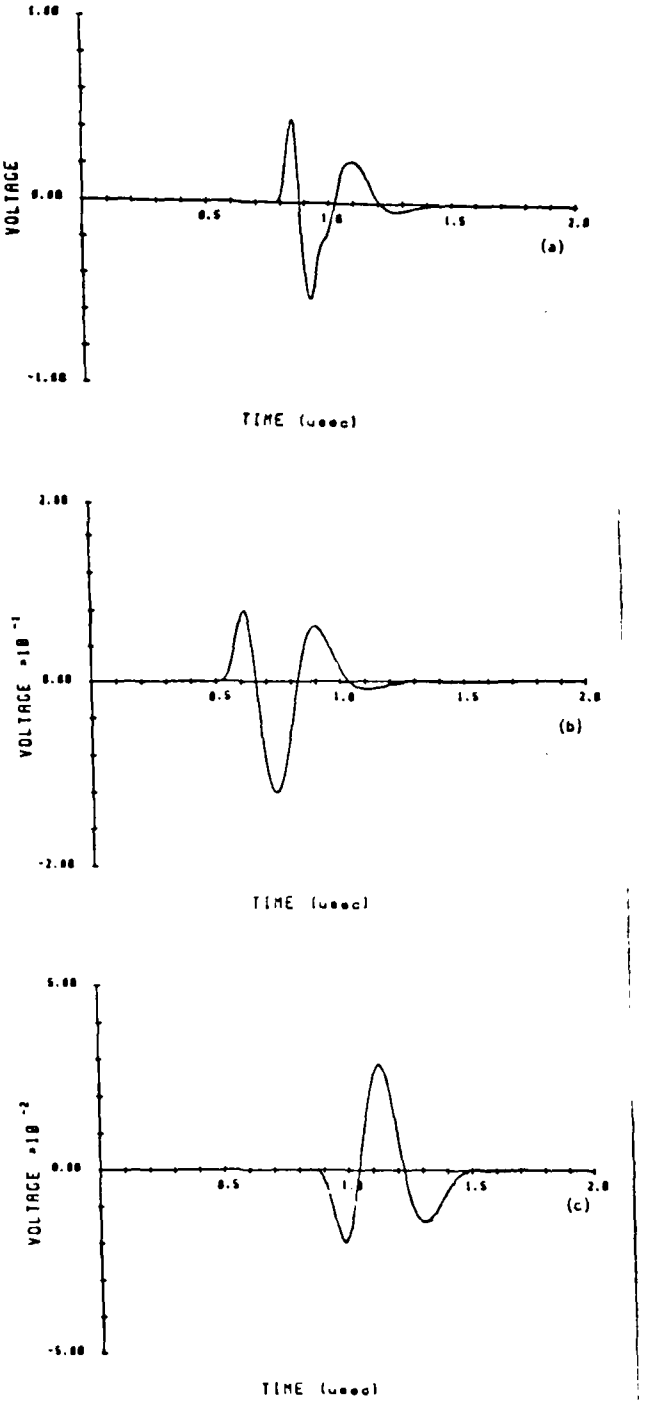

Figure 5. Buffer-rod-specimen signals of pure epoxy specimen for attenuation measurement: (a) echo A. (b) echo B, (c) echo C.

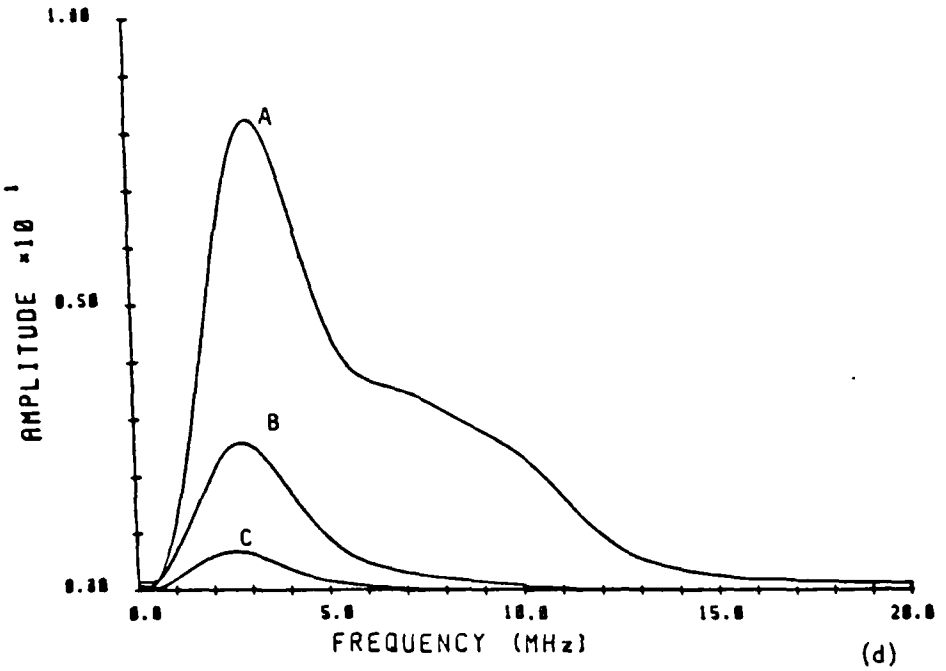

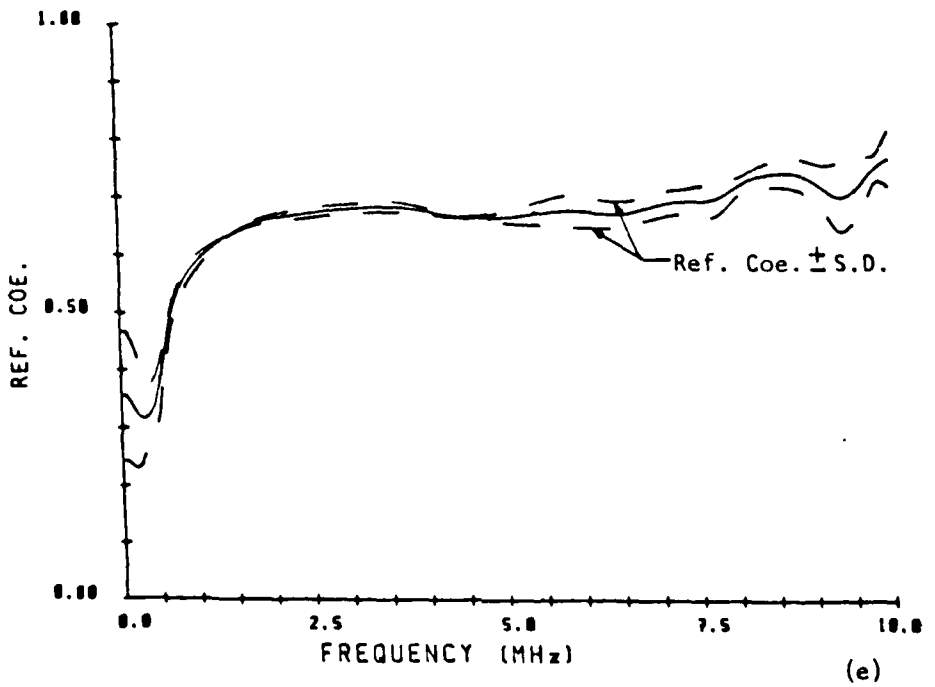

Figure 5. (d) Fourier amplitude spectra of echos A, B, and C, (e) reflection coefficient and ref. coe. ± S.D..

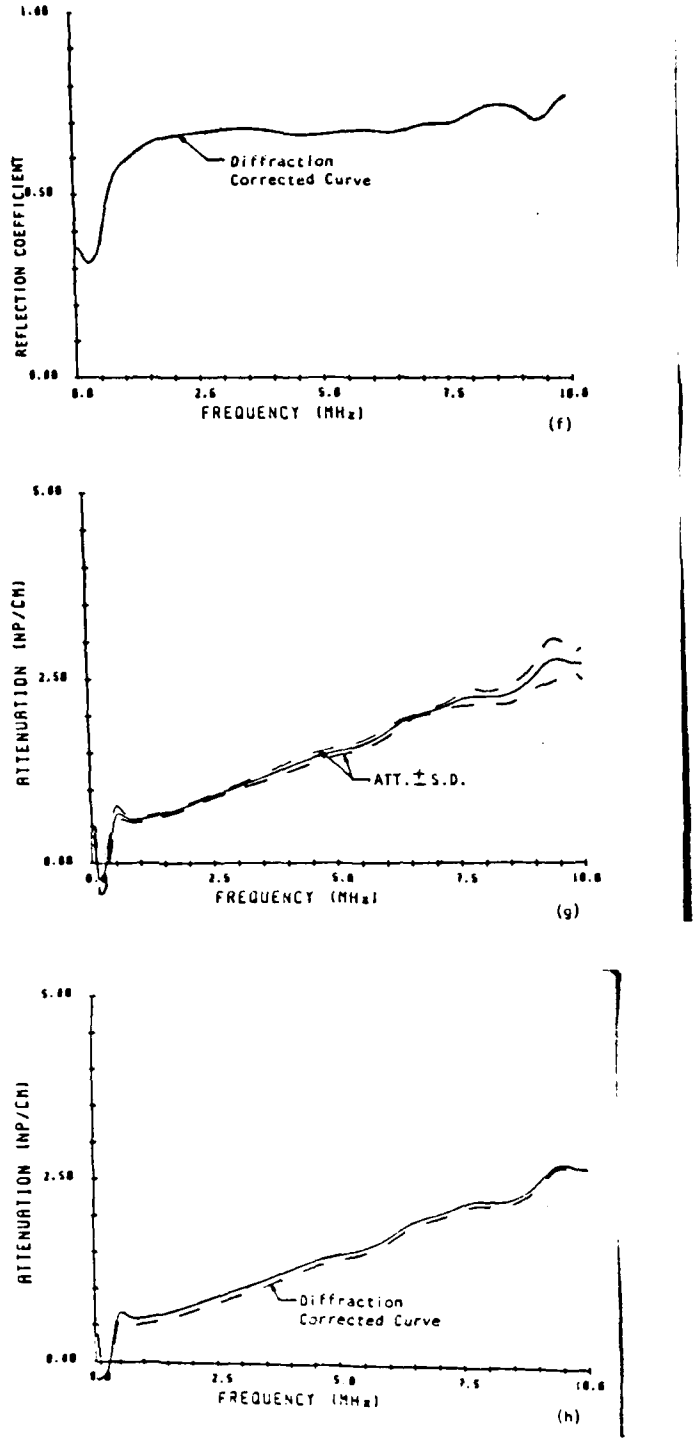

Figure 5. (f) reflection coefficient with and without diffraction correction, (g) attenuation and att. ± S.D.. (h) attenuation and its diffraction corrected curve.

coefficient curve and its standard deviation curves are plotted in Figure 5(e). The reflection coefficient with and without diffraction correction are shown in Figure 5(f). This shows that the reflection coefficient is nearly unaffected by wave diffraction effects. The attenuation curve and its standard deviation curves are shown in Figure 5(g). The attenuation with and without diffraction corrections are shown in Figure 5(h).

An example of the results obtained with the continuous-wave, swept-frequency method is shown in Figures 6(a)-(e). The excitation signal, the received signal after propagating through the specimen and the deconvolved power resonance curve, effectively removing the effects of the transducer ad electronics, are shown in Figures 6(a)-(c). The attenuation and its standard deviation curves are shown in Figure 6(d). The standard deviation is much higher than that of the data taken by the broadband pulse/echo method. The attenuation and its diffraction corrected curve are in Figure 6(e).

The results obtained by each of the methods above show that the attenuation in un-reinforced epoxy specimens, increases with frequency. The diffraction-corrected, frequency-dependent attenuation obtained with each method is shown in Figure 7. These results show that the lowest attenuation is obtained with the buffer rod method. This result is in agreement with the work of Papadakis [4], and it appears to be the result of minimizing and accounting for transducer coupling losses. The attenuation measured with the continuous-wave technique is the highest. It is suspected that this results from the excitation of adjacent resonance peaks and, unfortunately, this effect is difficult to remove from the resonance data. The deviations between the results obtained via various attenuation measurement techniques increase

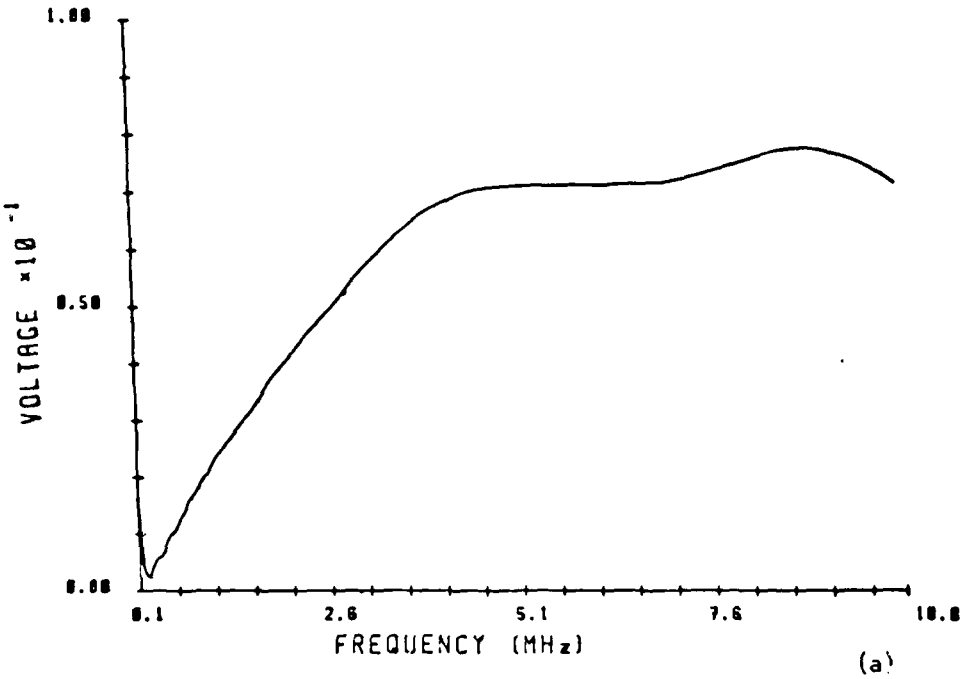

Figure 6. Continuous wave signals of pure epoxy specimen for atenuation measurement: (a) excitation signal.

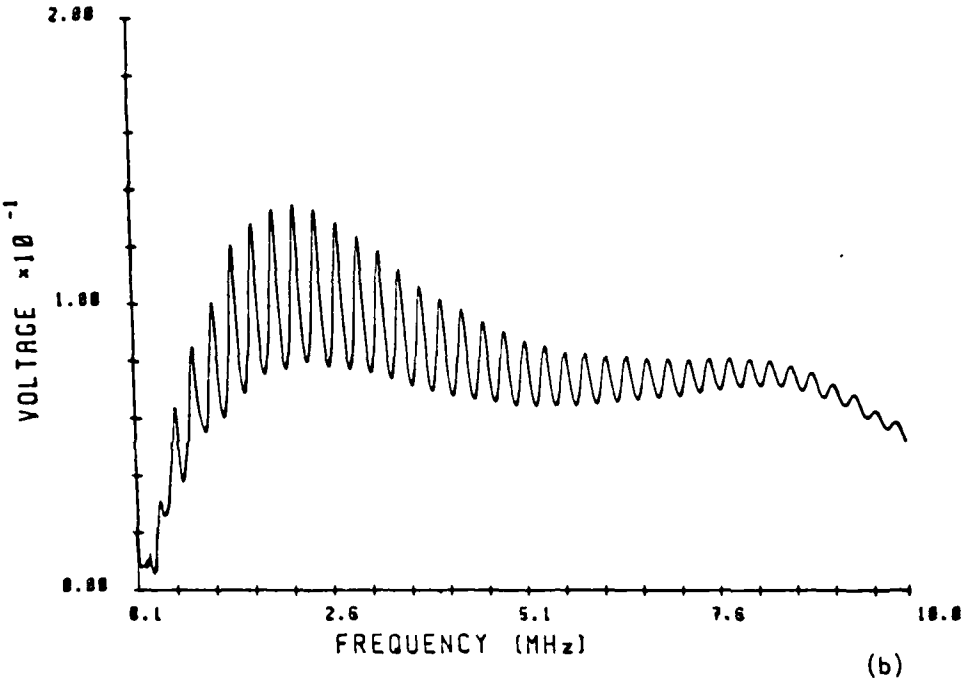

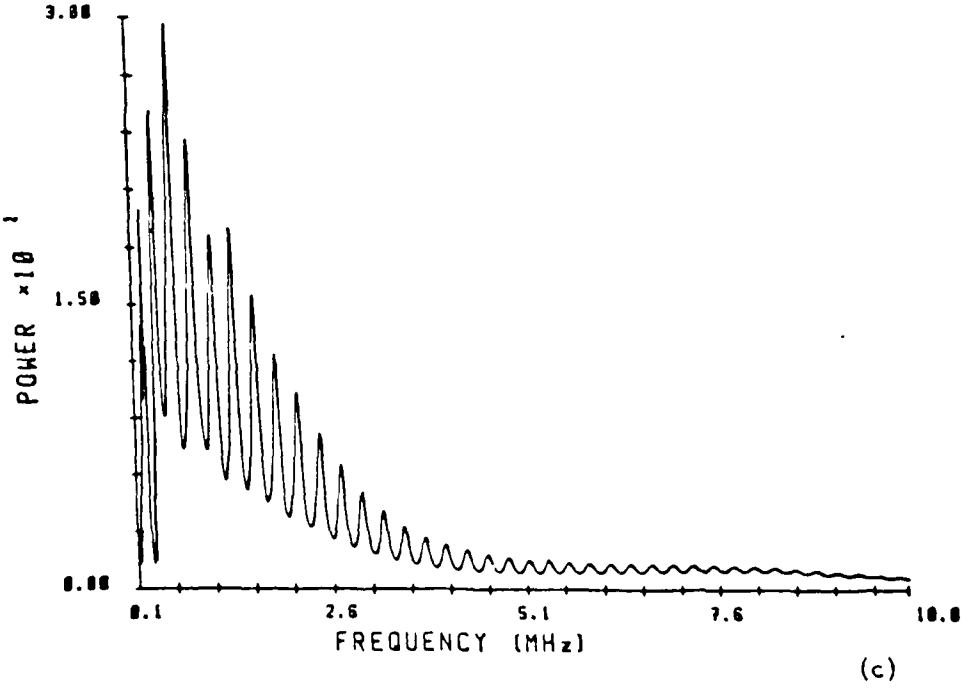

Figure 6. (b) signal passing through the specimen,
(c) deconvolved power resonance curve.

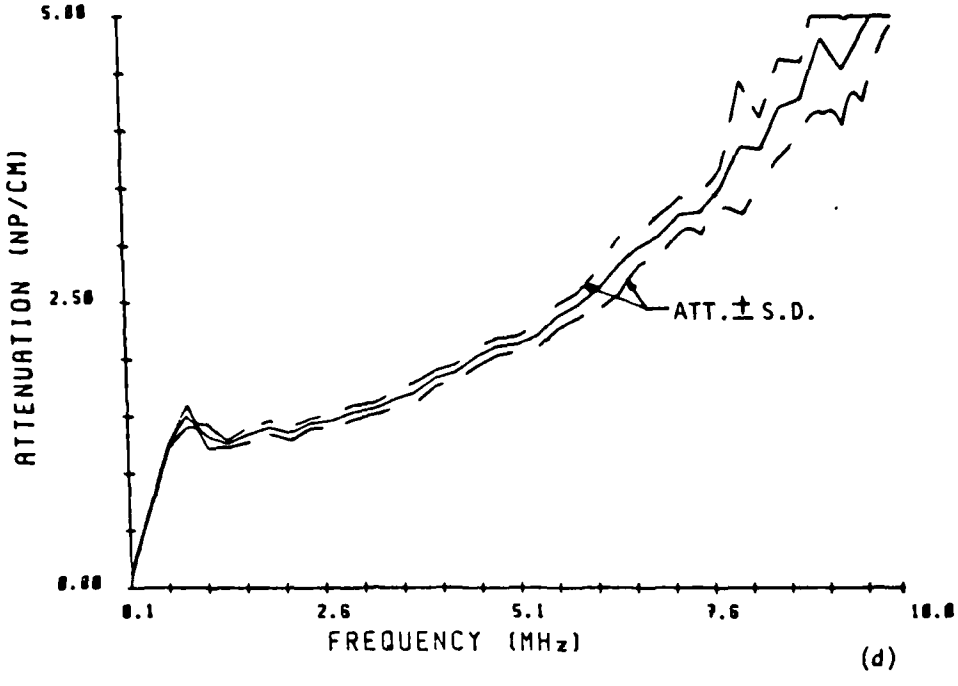

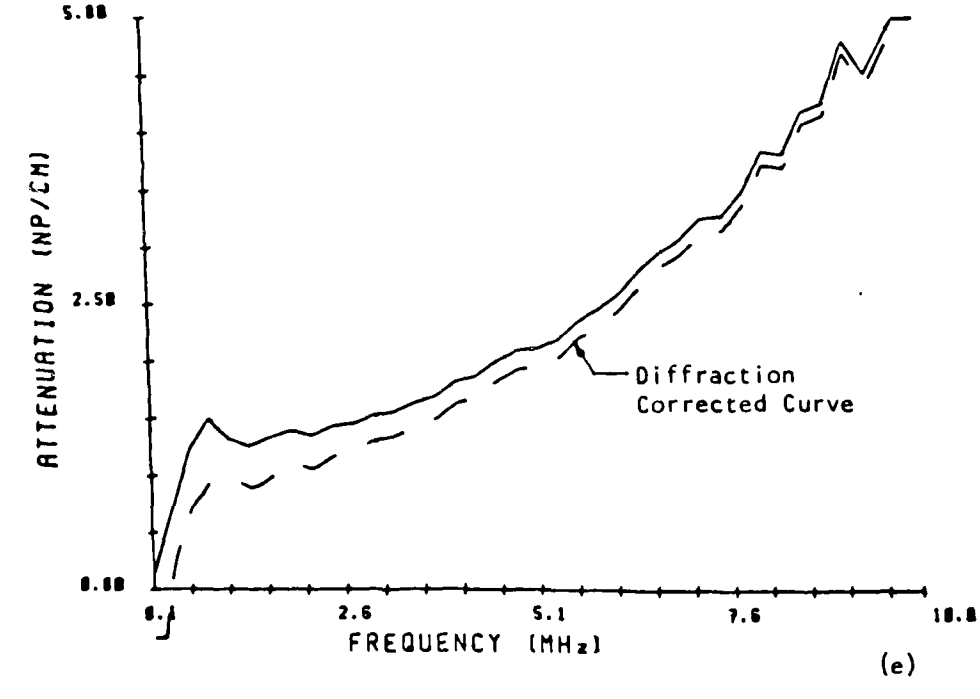

Figure 6. (d) attenuation and att. ± S.D.
(e) attenuation and its diffraction corrected curve.

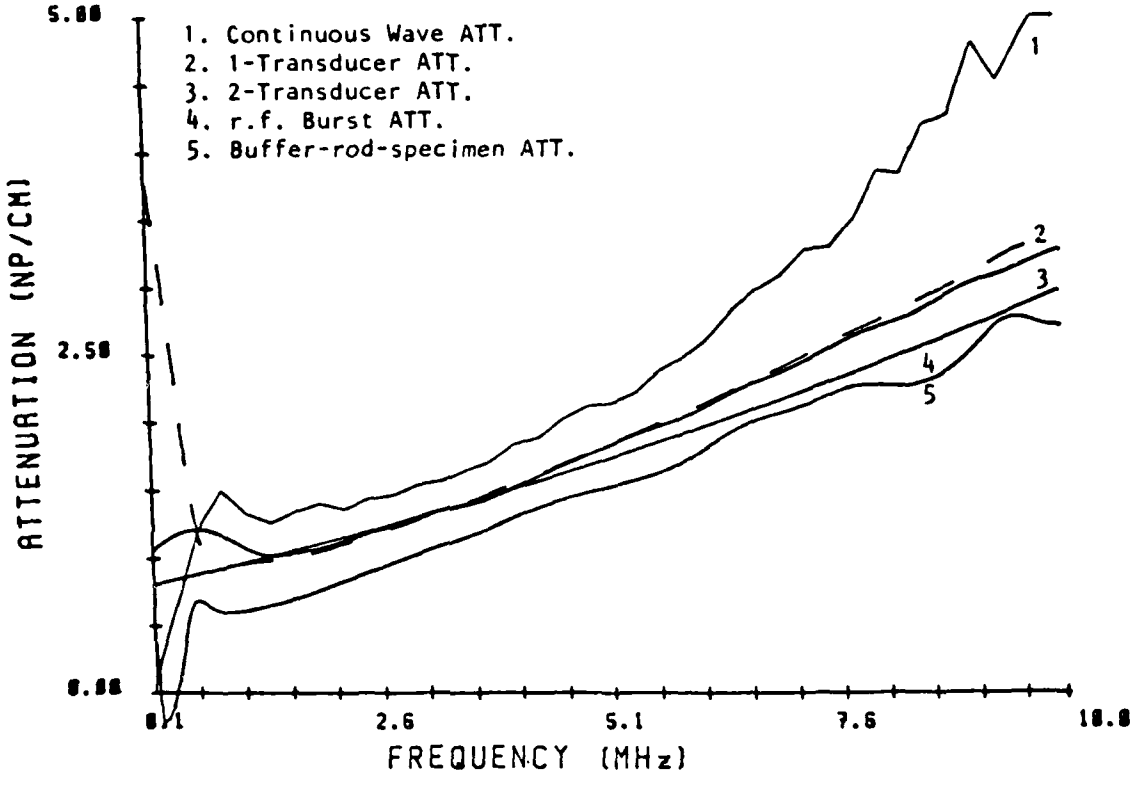

Figure 7. Overplotting of attenuation curves obtained from different ways. (pure epoxy specimen).

with increasing frequency. The reason for this was not established.

The attenuation obtained by the Hilbert-transformed dispersion data, with and without diffraction corrections, is shown in Figure 8. These results are typical and they show that the inclusion of diffraction corrections results in an even higher computed attenuation. At lower frequencies, the diffraction correction decreases the measured phase velocity values and the curvature of the diffraction-corrected phase velocity consequently increases. This results in a greater dispersion and this contributes, in turn, to a higher-valued attenuation curve.

4.2 Glass Laminated Specimens

The propagation of ultrasonic waves through multi-layer laminates fabricated of layers of glass and epoxy was investigated with the continuous-wave, swept-frequency technique. Microscope cover slides 1.2 mm thick were used to fabricate the laminates. The wavespeed of longitudinal waves in these pieces were measured to be 0.57 cm/μsec. From a wavelength analysis, it is found that the frequency interval Δf between "stop bands" should equal $\Delta f = c/2L$ or approximately 2.4 MHz for an infinite periodic structure fabricated of glass plates. The transmission coefficient is taken to be the amplitude ratio of signal transmitted through the laminate specimen and the input signal. The latter is obtained by putting source and receiving transducers in intimate contact. The logarithm of the transmission coefficients for specimens consisting of 1, 4, 6, 8 and 10 layers, measured in the frequency range from 0 to 10 MHz is shown in Figure 9. These curves demonstrate that the stop bands remain constant in number, but deepen as

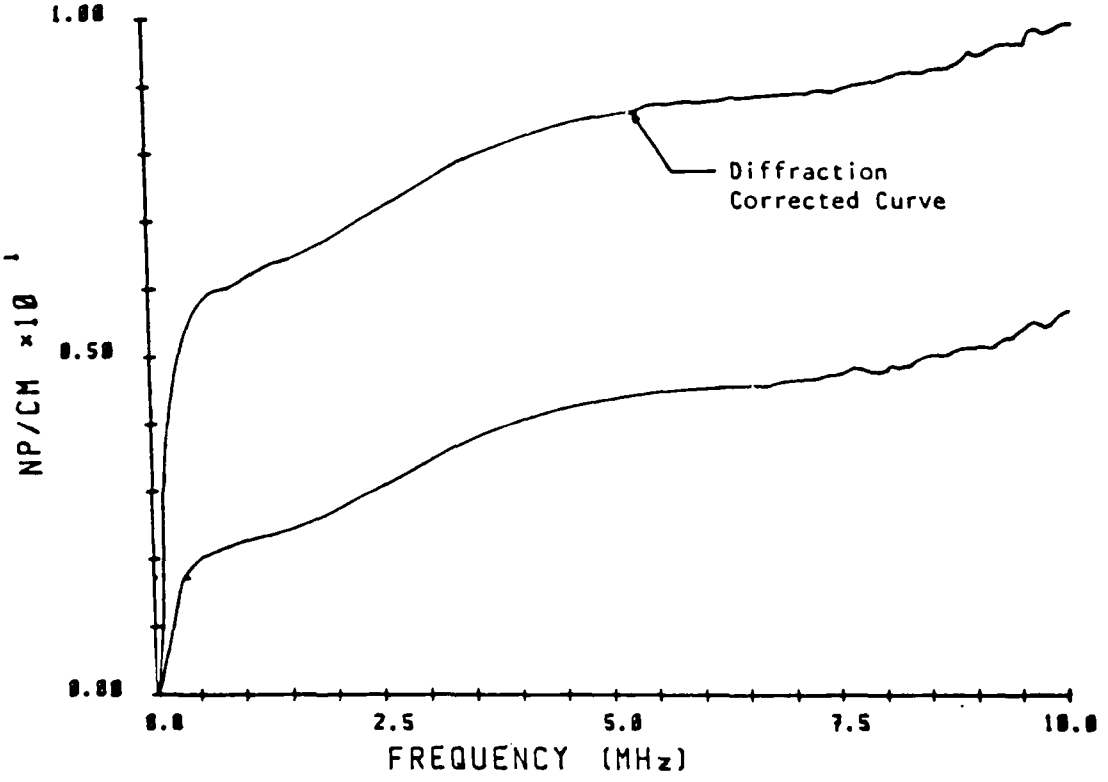

Figure 8. Hilbert transformed attenuation with and without diffraction correction.

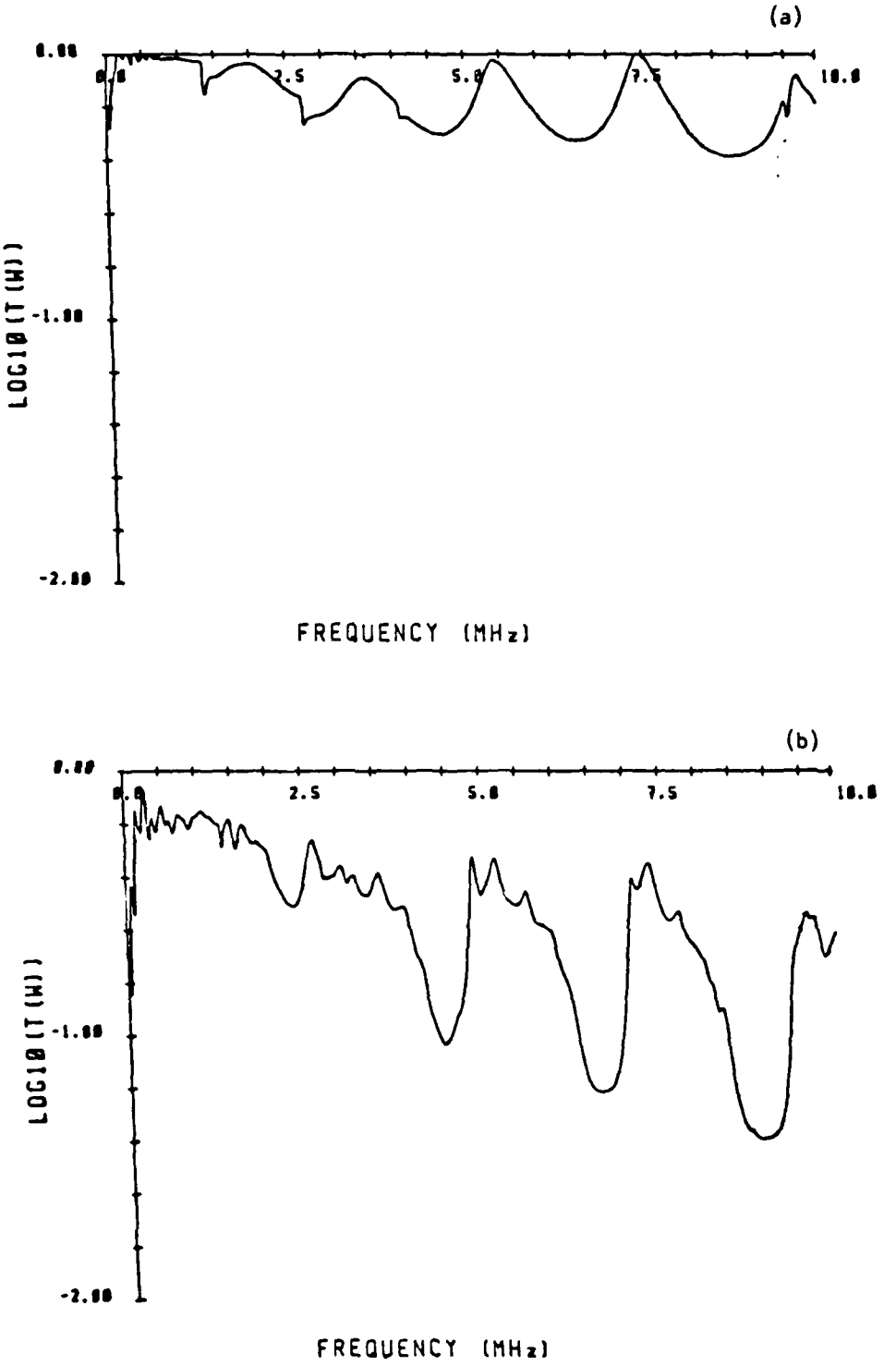

Figure 9. Stop band phenomenon of glass laminated specimen: (a) 1-glass layer specimen, (b) 4-glass layers specimen.

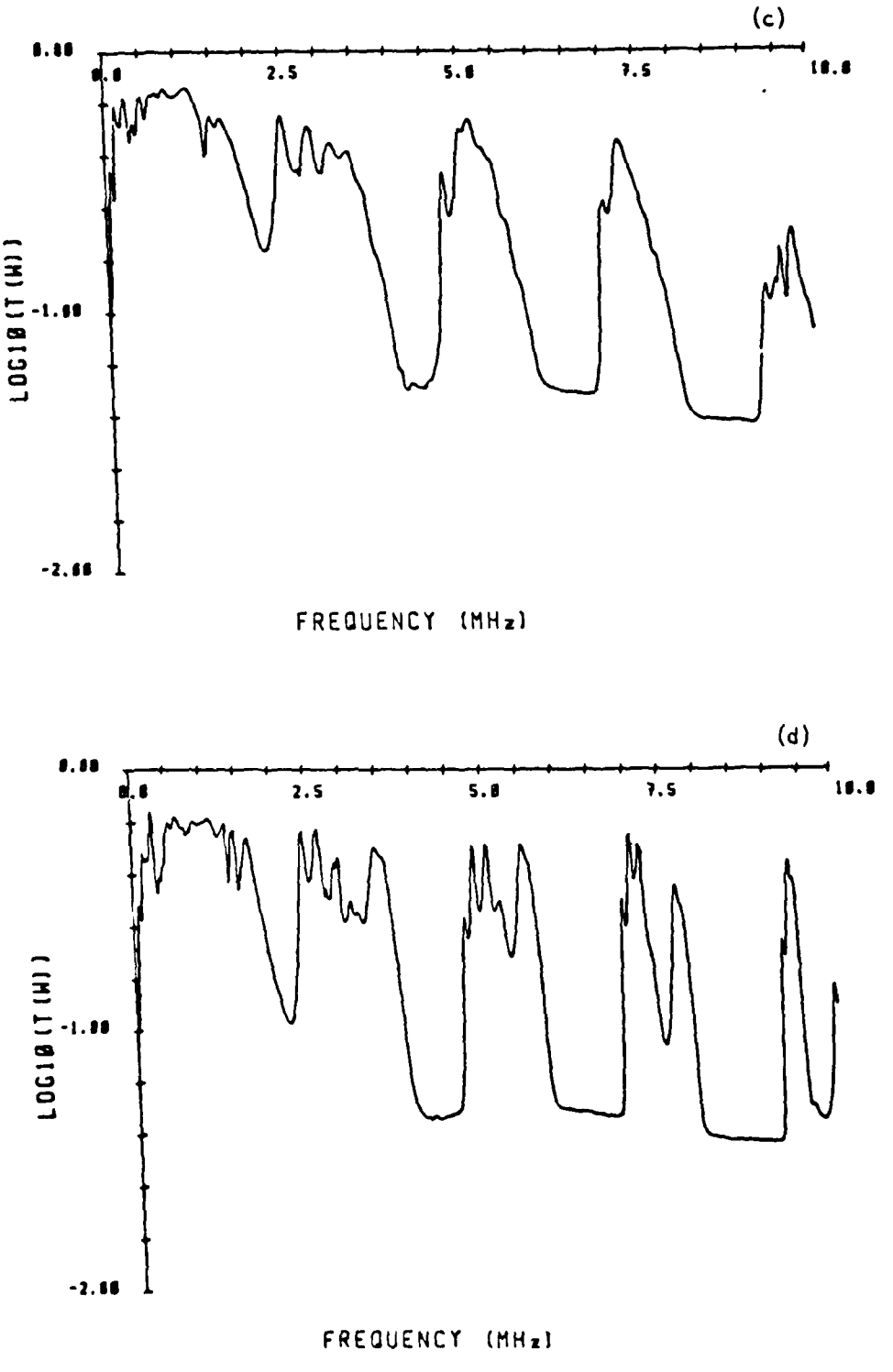

Figure 9. (c) 6-glass layers specimen, (d) 8-glass layers specimen.

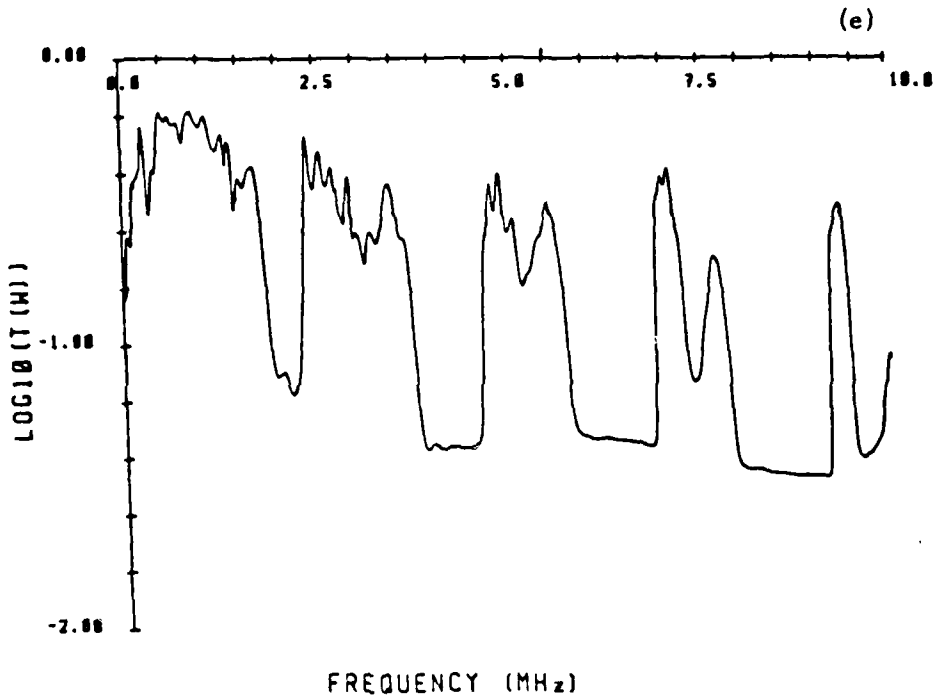

Figure 9 . (e) 10-glass layers specimen.

layers are added, producing frequency bands having increasingly high acoustic attenuation. The shallow, tightly spaced minima seen in these figures correspond to roughly the thickness resonance of the entire specimen. The numerical and experimental results obtained by Scott [5] are very similar to these experimental results.

4.3 32-ply Graphite/Epoxy Specimens: Thermal Cycling Effects

Ultrasonic measurements were competed on specimens of 32-ply graphite/epoxy which were thermally cycled. As in the previous work, the graphite/epoxy specimens were typically 0.175 in (0.445 cm) thick which restricted the ultrasonic measurements that could be made to a direction normal to the ply-layers. This coincides with the UT field inspection configuration. The imposed thermal treatment ranged from cooling by immersion in liquid nitrogen at -320°F (-196°C) to heating in boiling water at 212°F (100°C). After a number of repeated thermal heating/cooling cycles, the specimens were permitted to equilibrate to room temperature where the ultrasonic measurements were made.

The various ultrasonic techniques were applied to measure the phase velocity and attenuation as a function of frequency with thermal cycle number as a parameter. The diffraction loss and phase correction curves for isotropic materials were used as a first order approximation for correcting the measurements.

(1) Phase velocity - A typical input signal and the signal propagating through

a graphite-epoxy specimen are shown in Figures 10(a) and (b), respectively. The phase velocity curve obtained via Eq. 2 and its diffraction-corrected curve are shown in Figure 10(c). The difference between the phase velocity measured initially and that measured after 17 and 67 thermal cycles are shown in Figures 10(d). It is clear from this, that the frequency-dependent phase velocity is almost unchanged with this number of thermal cyclings. There was measured, however, a clear decrease in phase velocity relative to its value prior to thermal cycling. This effect is, however, small in comparison with the measured phase velocity variation among all the specimens prior to any thermal cycling, which is three times greater!

(2) Attenuation - The ultrasonic measurements were first used to investigate the "stop band" phenomenon. The measurements were made with broadband ultrasonic pulses. As before, the transmission coefficient was computed by dividing the Fourier amplitude spectra of the signals transmitted through the specimen by the spectrum of the input signal . The logarithm of the transmission coefficient for a 32-ply laminate of graphite-epoxy is shown in Figure 11. The first "stop band" is expected at about 11 MHz. The experimental results shown in Figure 11 exhibit a much higher attenuation at frequencies near 11 MHz which may be the result of the "stop band" phenomenon.

Based on the measurements on pure epoxy, because of the least transducer coupling losses, the attenuation measured from the buffer rod method was expected to yield the best results. It was found that this method is however difficult to apply to the graphite/epoxy specimens. The source of this difficulty lies in the rough specimen surface which results in excess scattering of the sound wave at the glass-specimen interface. For this

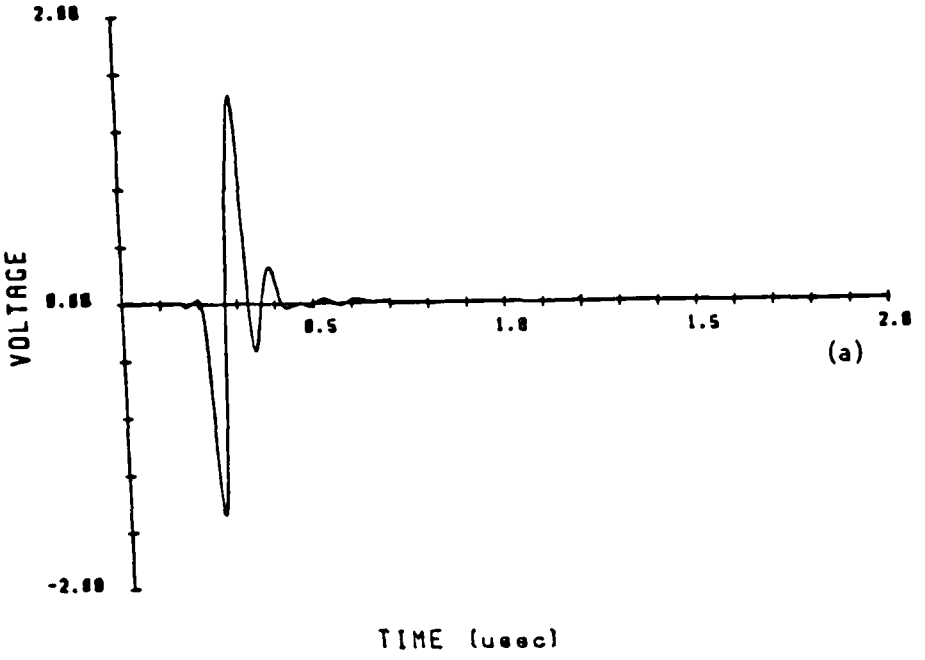

Figure 10. Signals of 32-ply graphite/epoxy specimens for phase velocity measurement: (a) excitation signal.

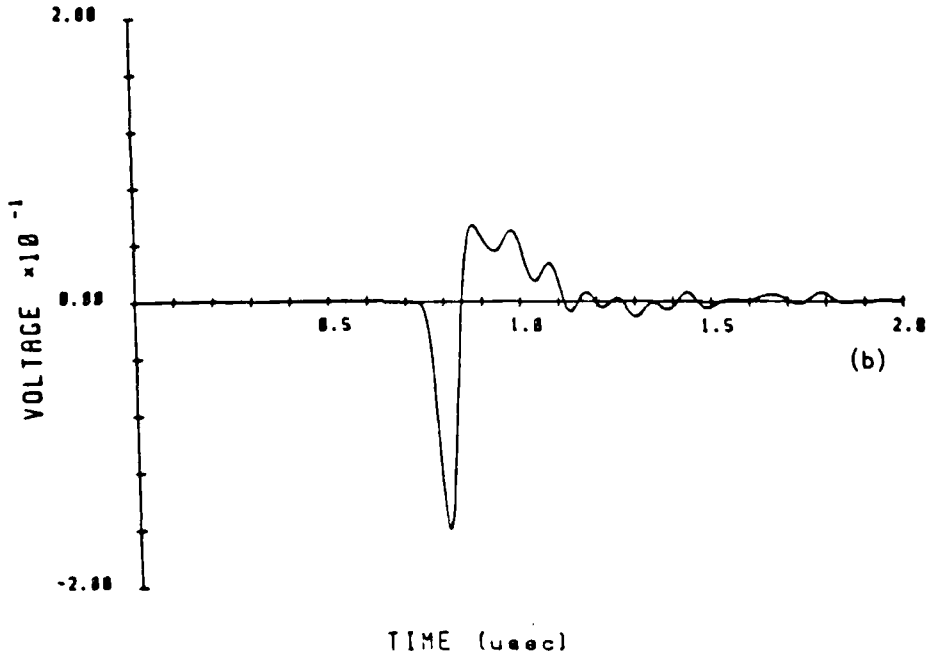

Figure 10. (b) delayed signal through the specimen,

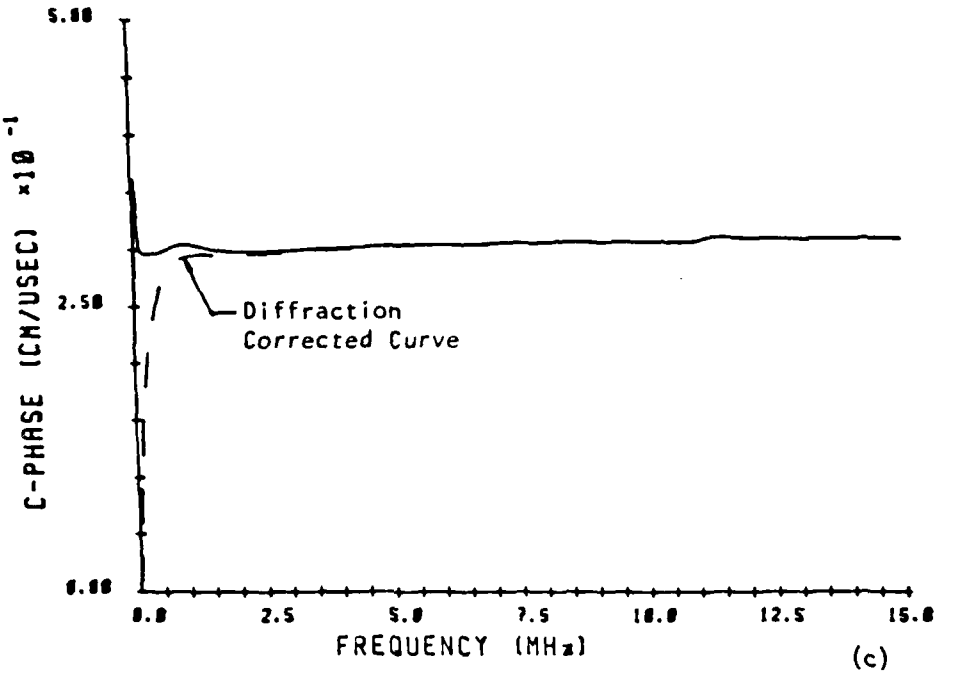

(c) phase velocity and its diffraction corrected curve.

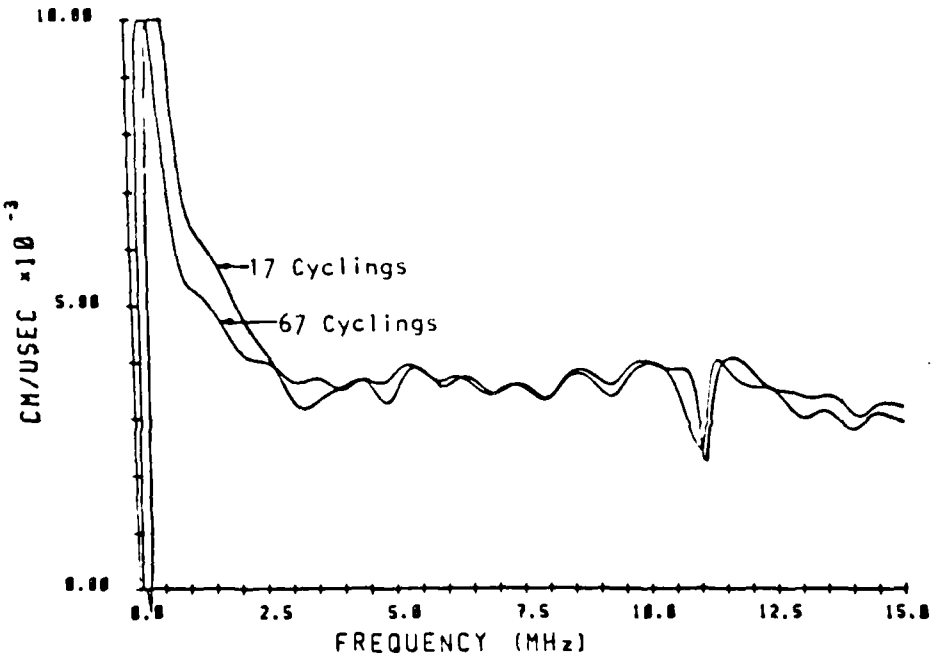

Figure 10. (d) the difference of phase velocity measured before and after thermal cyclings.

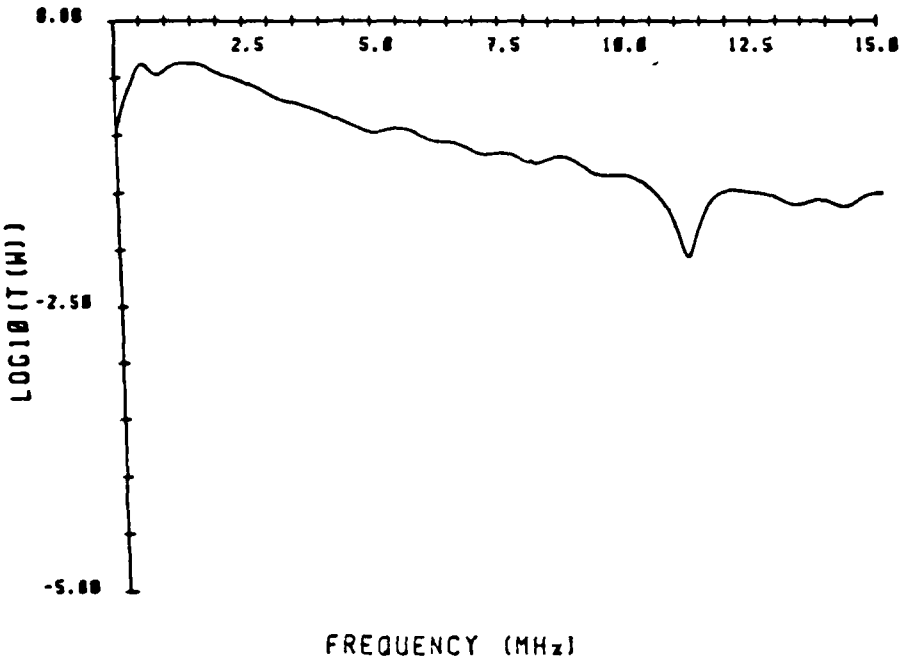

Figure 11 Stop band phenomenon of 32-ply graphite/epoxy specimen.

reason, the buffer rod method was abandoned.

From measurements with narrow-band r.f. burst signals, it was found that the echos were distorted by superimposed, low frequency signals. This made the measurement of the time domain amplitudes of the echos inaccurate and irreproducible.

In the following, the results of the measurements obtained using the broadband pulse and continuous-wave techniques will be summarized. The one-transducer (1/4 inch diameter) echos and their Fourier amplitude spectra are shown in Figures 12(a)-(c). The shallow, tightly spaced resonances appearing on the amplitude spectra curves correspond to the thickness resonances of the specimen. The attenuation measured before and after the thermal cyclings is graphed with their standard deviation curves in Figures 12(d)-(f). A typical attenuation curve and its diffraction-corrected curve are shown in Figure 12(g). The diffraction-corrected attenuation curves measured before and after thermal cyclings are plotted together for comparison in Figure 12(h). A similar series of the attenuation curves measured with the through-transmission technique and the continuous-wave method, using the same transducer as above, are shown in Figures 13(a)-(g) and 14(a)-(g). The Hilbert transform technique was also implemented to calculate the attenuation. The attenuation with and without diffraction-correction prior to thermal cycling is shown in Figure 15(a). The higher attenuation curve is obtained from the diffraction-corrected dispersion curve. The diffraction-corrected, Hilbert-transformed attenuation curves before and after thermal cyclings are plotted in Figure 15(b). The effect of thermal cycling temperature limits is undetermined in these tests and requires additional work.

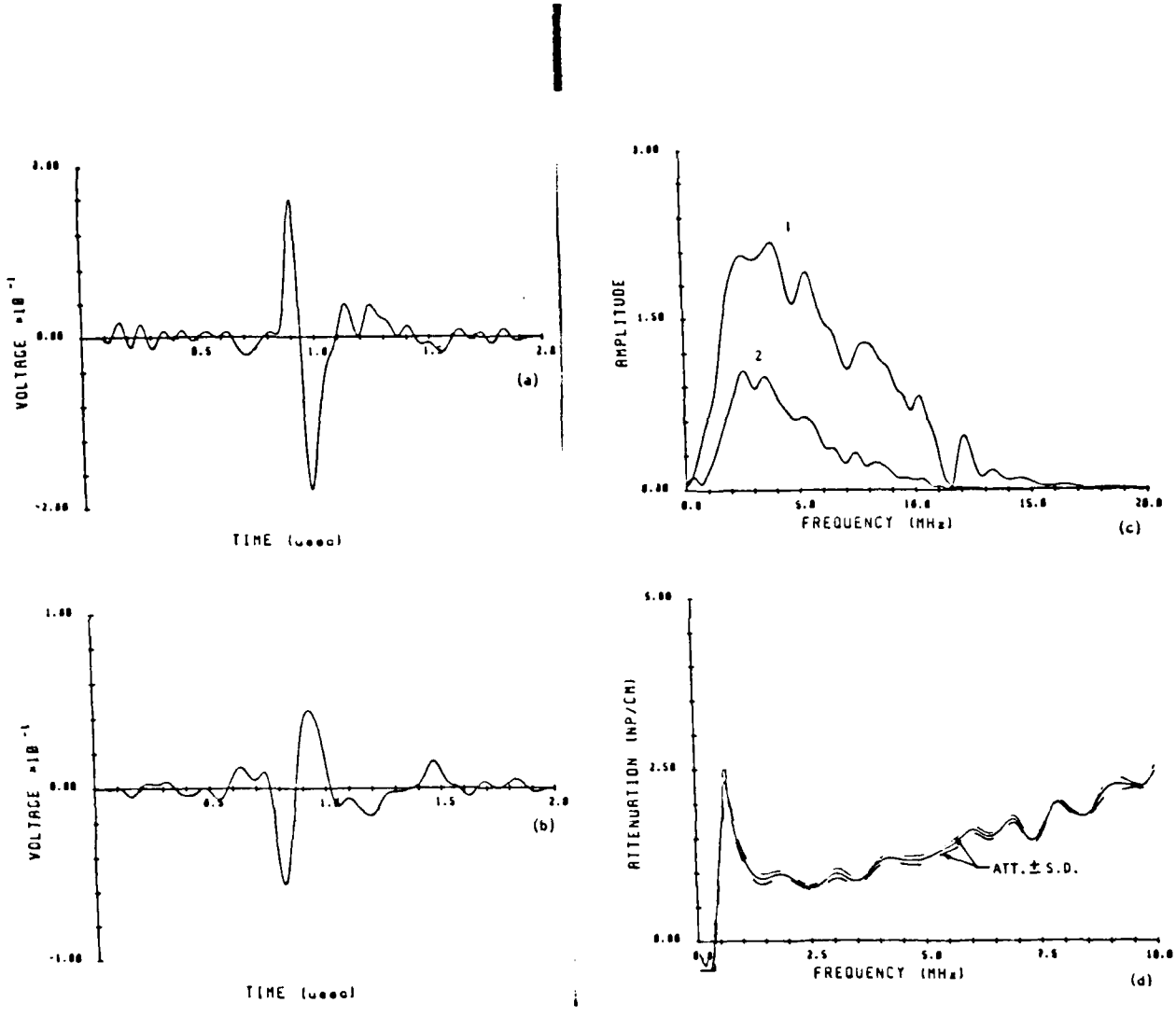

Figure 12. 1-transducer (1/4 inch diameter) signals of 32-ply graphite /epoxy specimen for attenuation measurement: (a) echo 1, (b) echo 2. (c) Fourier amplitude spectra of echo 1 and 2, (d) attenuation and att. ± S.D..

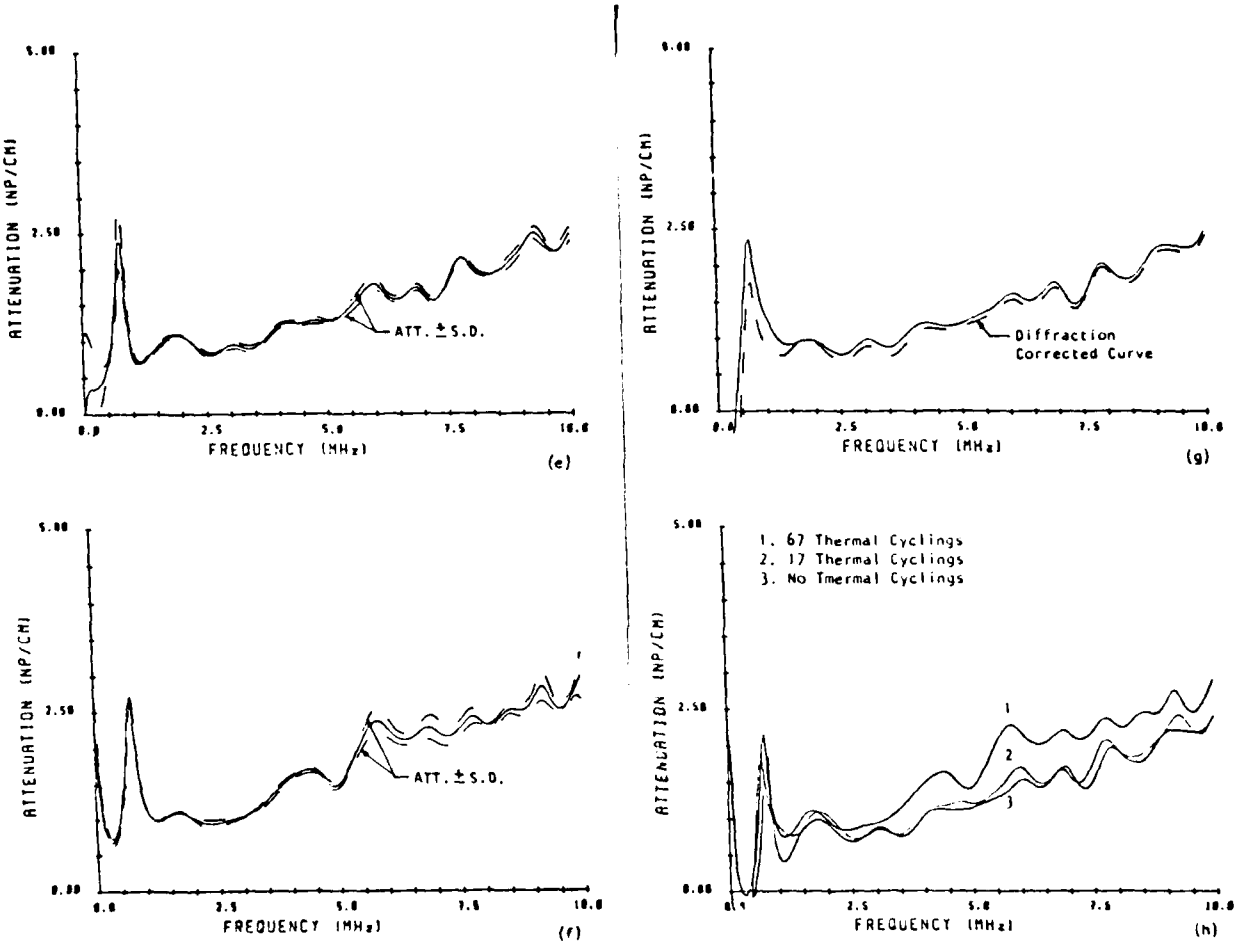

Figure 12. (e) 17 thermal cyclings attenuation and att. ± S.D.,
(f) 67 thermal cyclings attenuation and att. ± S.D..
(g) attenuation and its diffraction corrected curve,
(h) overplotting of attenuation curves obtained before and after thermal cyclings.

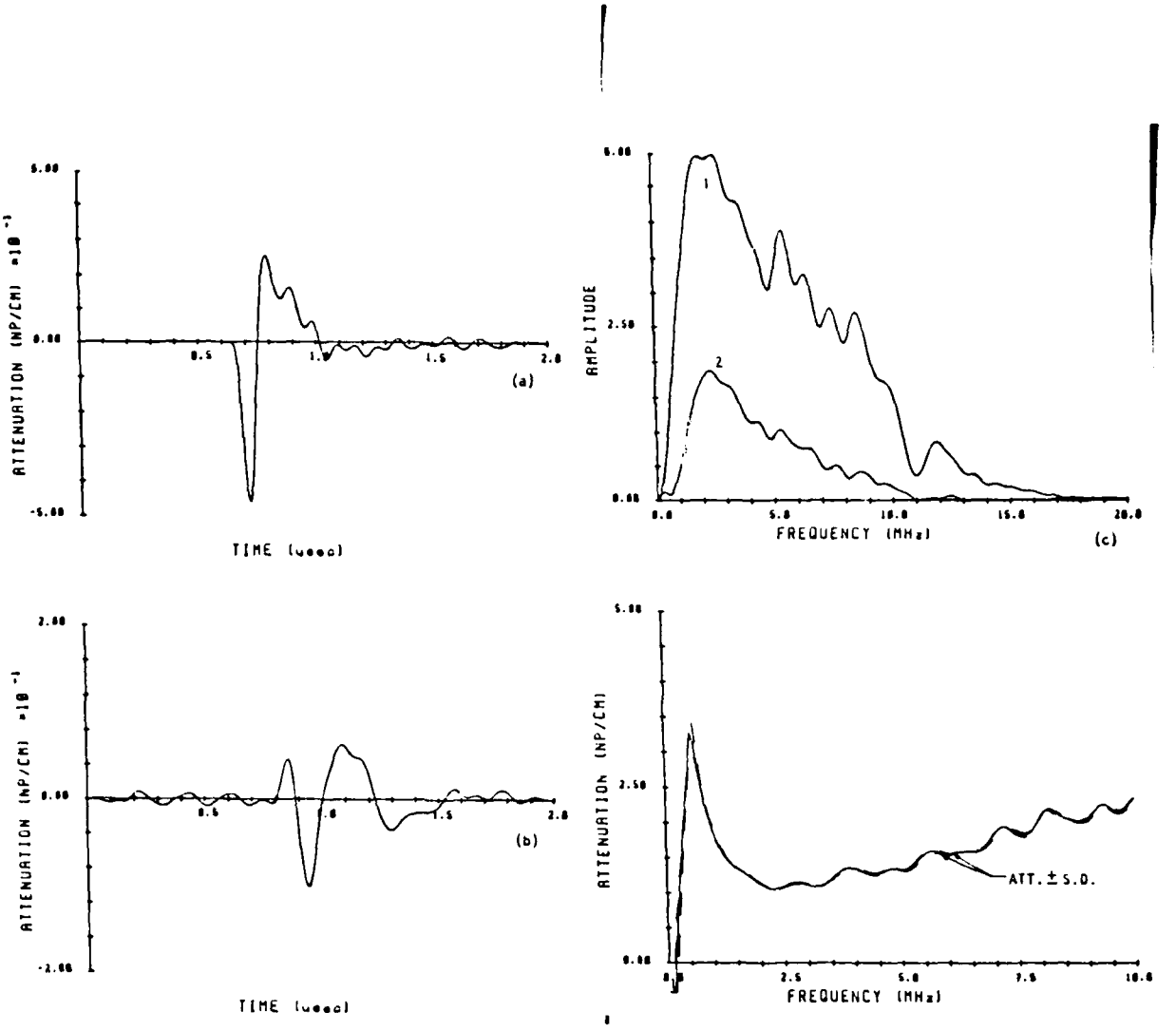

Figure 13. Through transmission (1/4 inch diameter transducer) signals of 32-ply graphite/epoxy specimens for attenuation measurement: (a) echo 1, (b) echo 2.
(c) Fourier amplitude spectra of echo 1 and 2,
(d) attenuation and att. ± S.D..

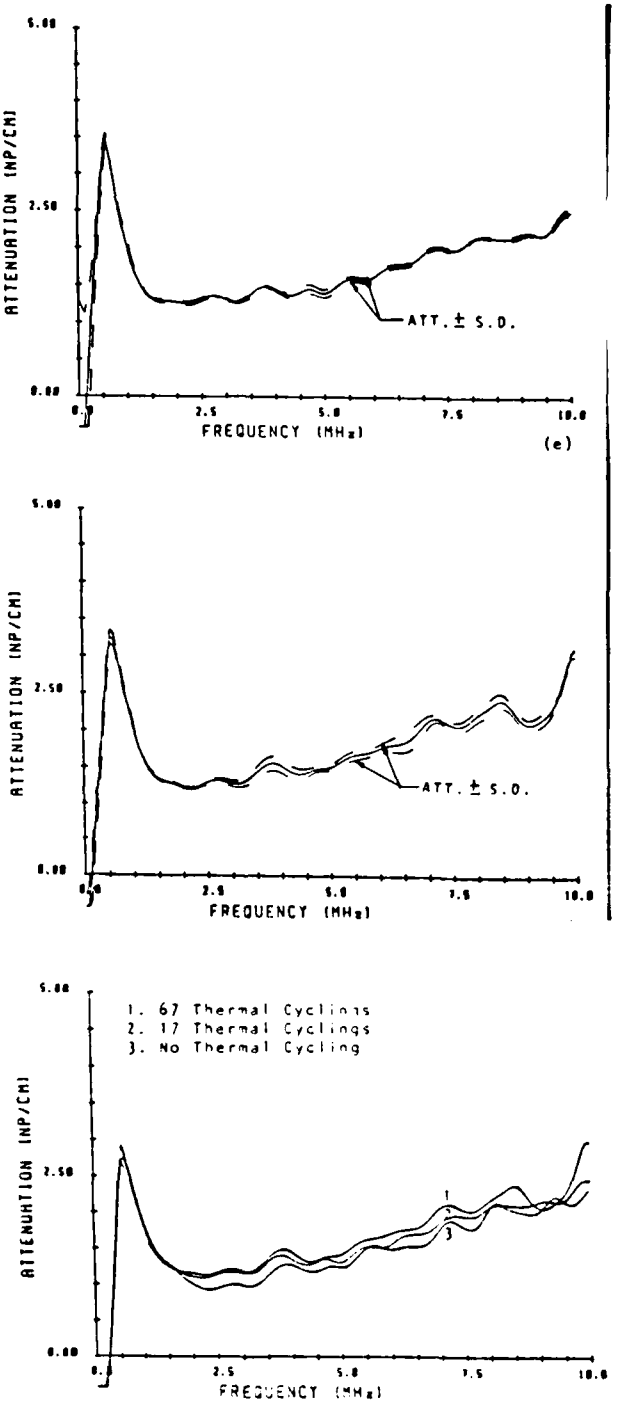

Figure 13. (e) 17 thermal cyclings attenuation and att. ± S.D.,
(f) 67 thermal cyclings attenuation and att. ± S.D..
(g) overplotting of attenuation curves obtained before and after thermal cylings

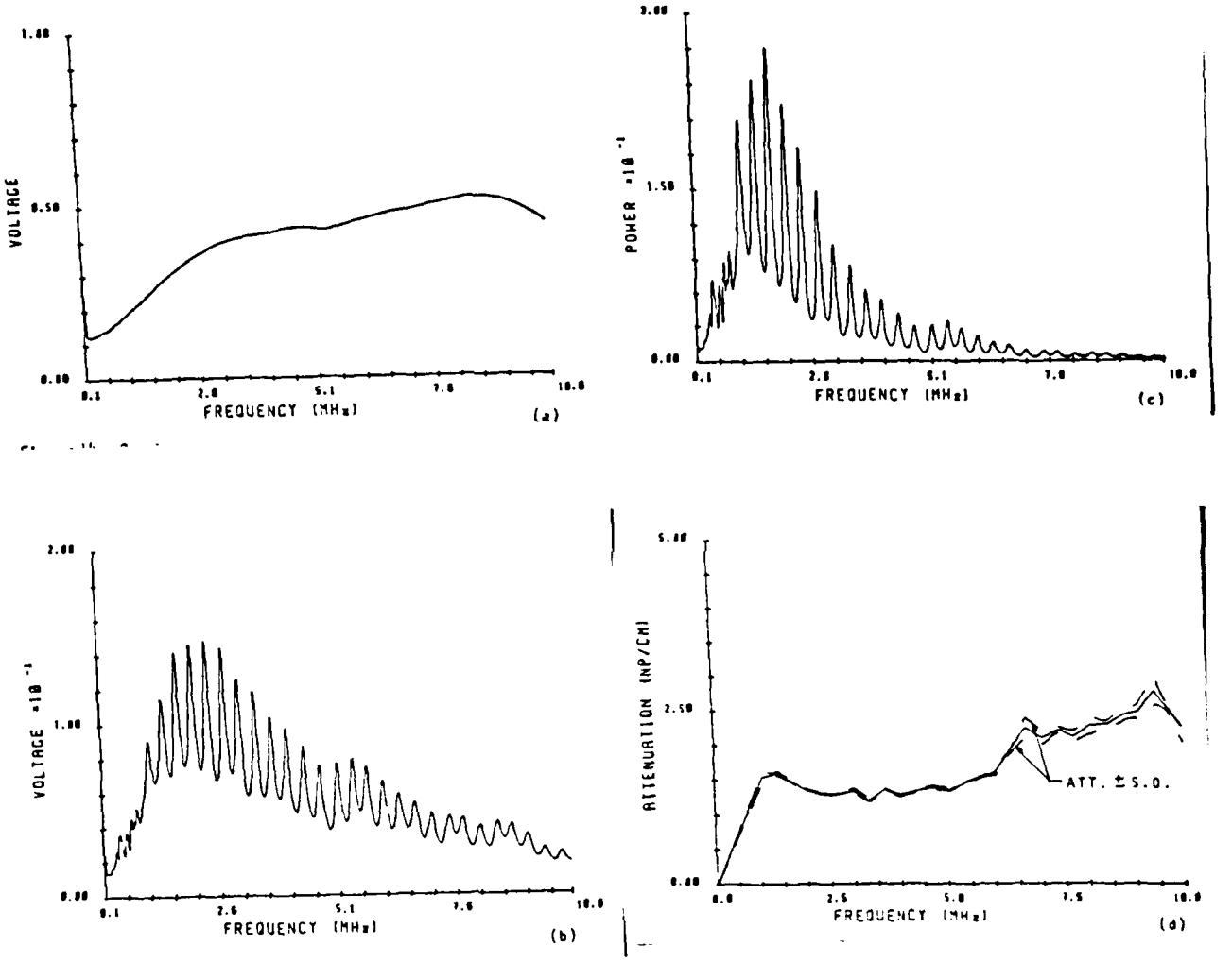

Figure 14. Continuous wave signals of 32-ply graphite/epoxy specimens for attenuation measurement: (a) excitation signal.
(b) the signal passing through the specimen,
(c) deconvolved power resonance curve.
(d) attenuation and att. ± S.D.,

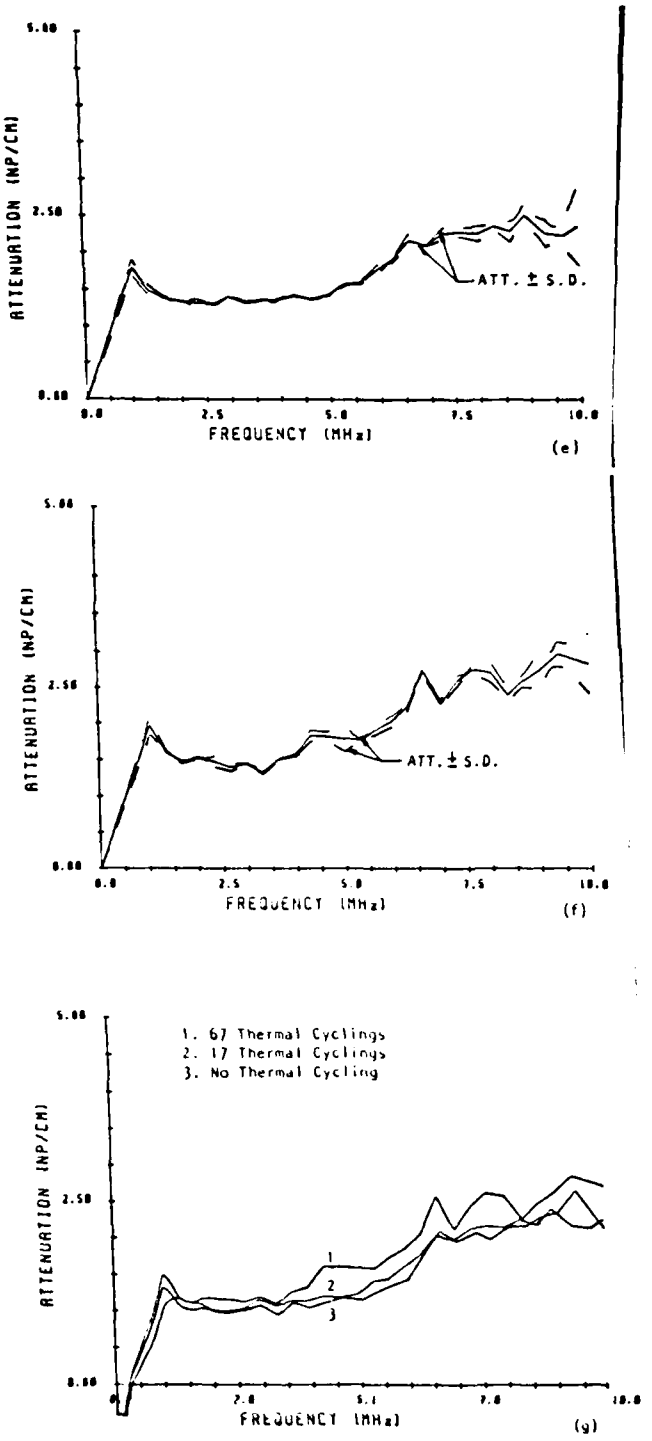

Figure 14. (e) 17 thermal cyclings attenuation and att. ± S.D..
(f) 67 thermal cyclings attenuation and att. ± S.D.,
(g) overplotting of attenuation curves obtained before and after thermal cyclings.

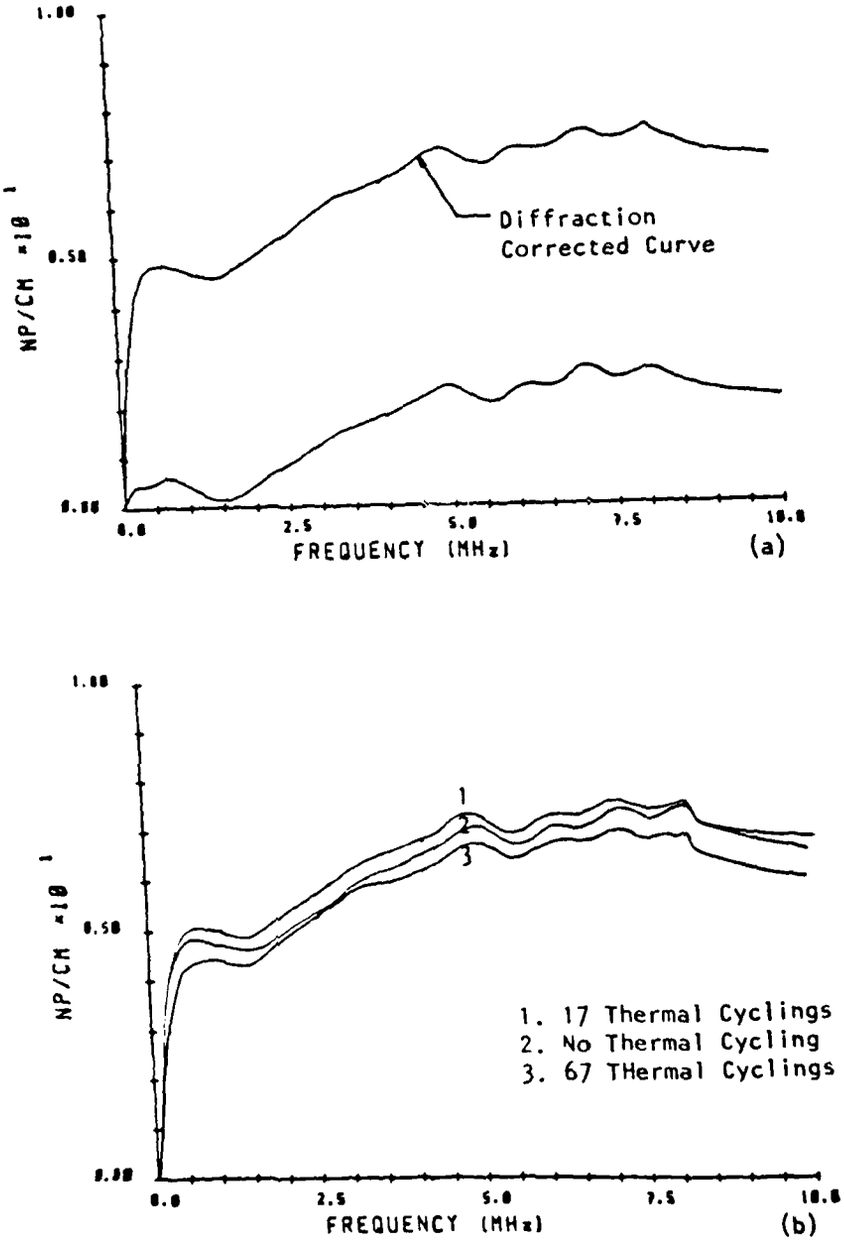

Figure 15. (a) Hilbert transformed attenuation with and without diffraction correction, (b) overplotting of Hilbert transformed attenuation with diffraction correction before and after thermal cyclings.

All the attenuation data prior to thermal cycling the specimen, except for that determined by the Hilbert transform technique, is plotted together in Figure 16. These curves show that the differences among the attenuation data obtained by the various techniques are of the same order as the change of attenuation after thermal cycling. Furthermore, the variation of attenuation measured by the same transducer on the same specimen but at different times over a period of six months, exhibits a similar variation.

After thermal cycling the composite specimens, microcracks could be seen even at low magnifications on the surfaces of the specimens along the fibers, across the entire specimen width. A micrograph of such a specimen is shown in Figure 17. In one series of measurements, after 17 thermal cyclings, there were eight microcracks (0.44 cracks/cm^2) on one side of the specimen and ten (0.56 cracks/cm^2) on the other side. After 67 cycles, the crack number on each side increased to ten (0.56 cracks/cm^2) and sixteen (0.9 cracks/cm^2), respectively. The increment of attenuation might be related to the microcracks generated not only on the surface of the specimens but also in their interior.

These results again demonstrate that in cases where the wavelength of the ultrasonic waves used to make the inspection is more than twice the thickness dimension of a layer, the influence of the cracks to both the phase velocity and attenuation is very small.

4.4 Deformation Effects in Graphite/Epoxy Specimens

The through-transmission technique was used with 0.5 inch (1.27 cm)

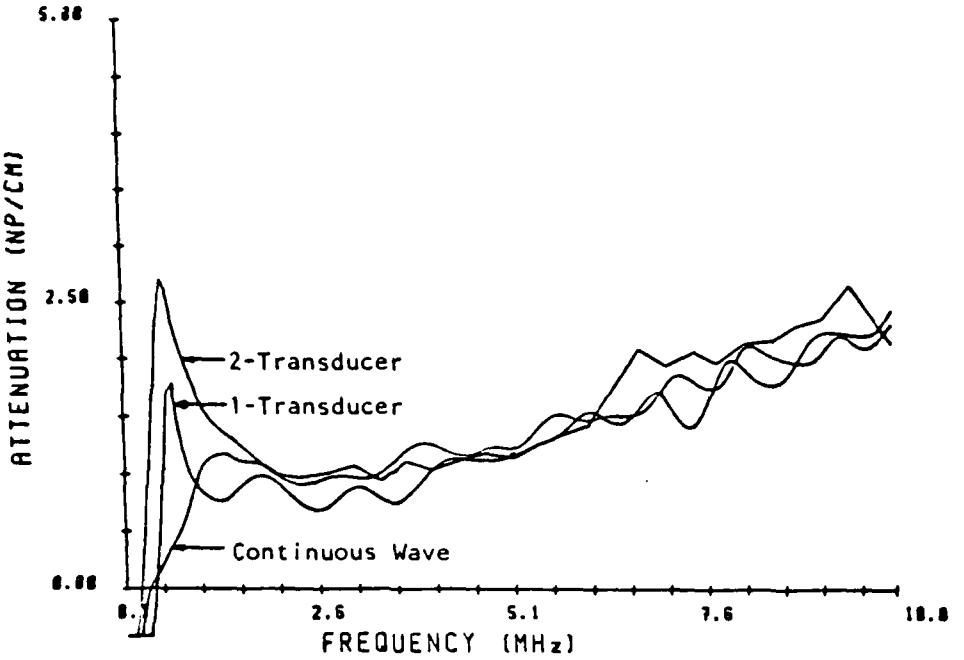

Figure 16. Overplotting of attenuation curves obtained from different ways before thermal cyclings.

Figure 17. Microcrack generated after thermal cyclings. (Magnification = 665)

diameter transducers to measure the attenuation. A comparison of the attenuation was made on the specimen prior to its loading in a uniaxial tension test to failure. The attenuation curves are shown in Figure 18. As shown in the test, the attenuation of ultrasonic waves in composite specimen remains relatively constant with load to near failure. Furthermore, as these curves show, the frequency-dependence of the attenuation of the unloaded specimen is very similar to that of a specimen under 3.0 kips load, that is, the attenuation shows only a slight increase with frequency between 1 and 10 MHz. The specimens were notched and typically began to fail in the notched region at 3.1 kips (22.8 ksi) and after failure, the load dropped to 2.5 kip (18.4 ksi). The long wavelength (two times the thickness of one layer) makes these measurements insensitive to the microstructural changes which are occurring on the ply-layer dimensional scale. This is in agreement with earlier measurements by Hsu and Tauchert in other composite specimens [6].

4.5 Conclusions

Several conclusions can be drawn from the work completed under this contract. From the analyses of waves through elastic and viscoelastic laminates, "stop bands" are expected in the dispersion curves and in the frequency-dependent attenuation curves. The attenuation curves show a marked increase in the "stop band". Furthermore, the analyses show that for laminates possessing slight irregularities in their spacing or in cases when some of the layers are viscoelastic, the boundaries of the "stop bands" become smoothed in the frequency domain. The experimental results obtained on glass/epoxy laminates exhibit the "stop band" phenomenon, but a critical

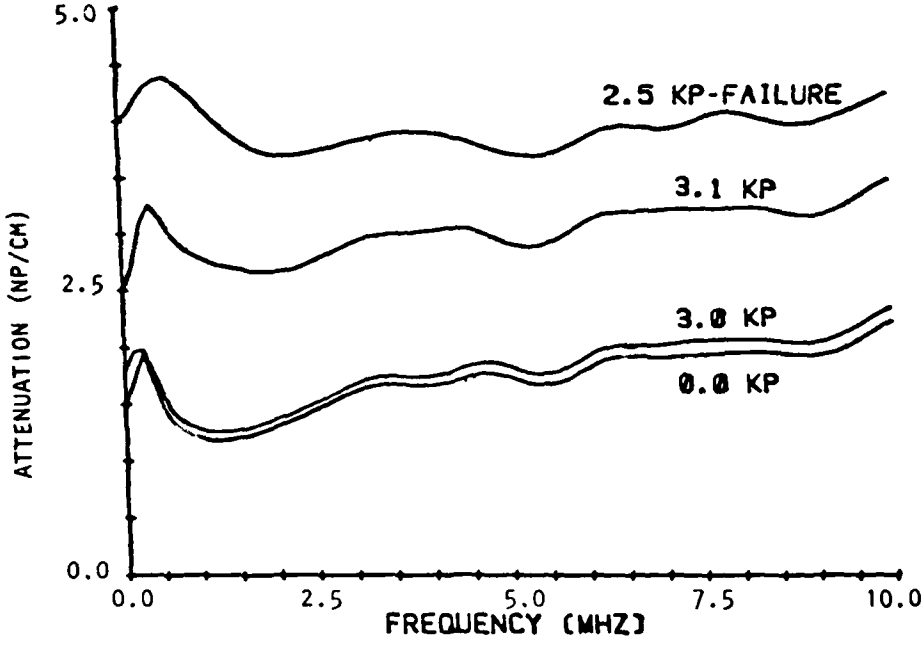

Figure 18. The attenuation of 32-ply graphite/epoxy specimen measured during uniaxial tension test.

investigation of the all the predictions of the theory was not possible because of specimen fabrication limitations.

The experimental techniques which were used in this work permit the accurate determination of the frequency-dependent dispersion relation, phase and group velocities and attenuation in a broad variety of composite and viscoelastic materials. A new, and initially very promising attenuation measurement technique, based on the Kramers-Kronig relations was developed theoretically and implemented in an ultrasonic measurement system. However, the attenuation measurements are only reproducible if they are made at one specific specimen location with one measurement technique. The measured dispersion effects in graphite/epoxy specimens in the frequency range between 1 and 10 MHz (extending possibly to 30 MHz) are slight. Ultrasonic phase velocity measurements appear to be insensitive to small changes in the microstructure of the composite specimens which accompany cyclic thermal treatments or mechanical loadings. The effects of such treatments only appear as small changes in the frequency-dependent attenuation. Unfortunately, as shown by the exhaustive measurements carried out under this project, the measured attenuation value (at one frequency or as a function of frequency) is dependent on the measurement technique used to determine it and it exhibits a variation which is far greater than the attenuation changes resulting from the mechanical or thermal treatments imposed on a specimen which result in clearly identifyable microstructural damage.

Based on our and other investigators' theoretical work, investigating the propagation of ultrasonic waves through a medium with a periodic structure, changes in the dispersion and frequency-dependent ultrasonic characteristics

of a composite are expected, when microstructural changes are occurring either in the matrix or fibers, or in the interface between these two components. The experimental aspect of this work has amply shown that at least in the frequency range normally used in ultrasonic inspection techniques, these microstructural changes do not appreciably affect the ultrasonic properties in an amount greater than the variation obtained among the various measurement techniques.

5.0 REFERENCES

1. W. Sachse and Y. H. Pao, "On the Determination of Phase and Group Velocities of Dispersive Waves in Solids", J. Appl. Phys., 49, 4320-4327 (1978).

2. W. Sachse, C.S. Ting and A. Hemenway, "Dispersion of Elastic Waves and Non-destructive Testing of Composite Materials", in Composite Materials: Testing and Design (Fifth Conference), ASTM STP 674, S.W. Tsai, Ed., Am. Soc. Test. Matls., Philadelphia (1979), pp.165-183.

3. G.C. Benson and O. Kiyohara, "Tabulation of some Integral Functions describing Diffraction Effects on the Ultrasonic Field of a Circular Piston Source", J. Acoust. Soc. Am., 55, 184-185 (1974).

4. E.P. Papadakis, "Ultrasonic Velocity and Attenuation: Measurement Methods with Scientific and Industrial Applications", Chapt. 3 in Physical Acoustics, Vol. XI, W.P. Mason and R.N. Thurston, Eds., Academic Press, New York, (1976), pp. 151-211.

5. W.R. Scott and P.F. Gordon, "Ultrasonic Spectrum Analysis for Nondestructive Testing of Layered Composite Materials", J. Acoust. Soc. Am., 62, 108-116 (1977).

6. N.N. Hsu and T.R. Tauchert, "Influence of Stress Upon Internal Damping in a Fiber Reinforced Composite Material", J. Comp. Matls, 7, 516-520 (1975).

6.0 PUBLISHED PAPERS, REPORTS AND PRESENTATIONS

The following papers and reports were written and presentations were made at scientific meetings during the duration of the contract (July 1, 1978 to February 28, 1982).

1. R. Weaver and Y.H. Pao, "Multiple Scattering of Waves in Irregularly Laminated Composites", J. Appl. Mech., 47, 833-840 (1980).

2. R.L. Weaver and Y.H. Pao, "Dispersion Relations for Linear Wave Propagation in Homegeneous and Inhomogeneous Media", J. Math. Phys., 22, 1909-1918 (1981).

3. W. Sachse and C.-P. Chen, "The Dispersion of Elastic Waves and the Non-destructive Testing of Composite Materials", in Paper Summaries, National Spring Conference, ASNT, Am. Soc. for Non-destructive Testing, Columbus, Ohio (1980), pp.149-152.

4. W. Sachse, "Ultrasonic Wave Dispersion and the Non-destructive Testing of Composite Materials", Paper read at the "DARPA/AFML Review of Progress in Quantitative NDE" meeting, La Jolla, Calif., July 1980.

5. C.-P. Chen, "Ultrasonic Velocity and Attenuation Measurements in Composite Materials", M.S. Thesis, Cornell University, Ithaca, New York (January 1983).

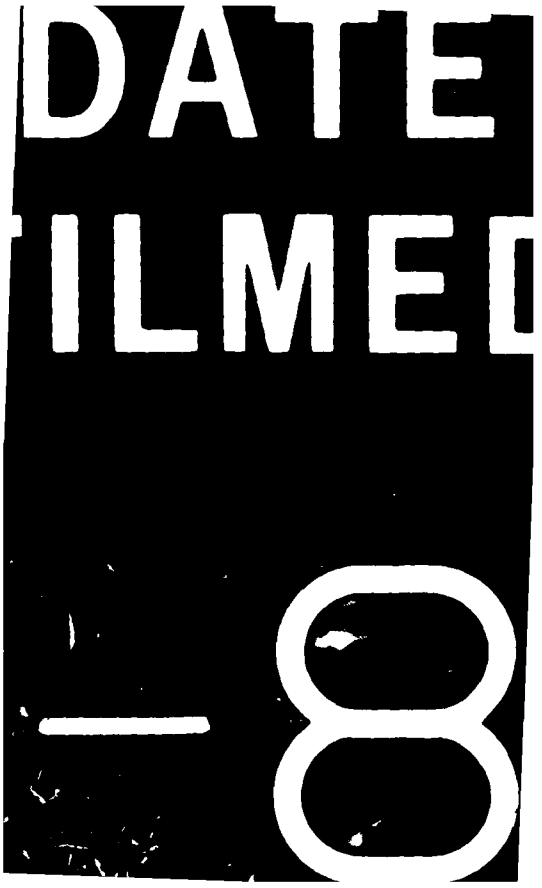
DATE
ILME
8